Peer-reviewed version available at Int. J. Mol. Sci. 2018, 19, 2231; doi:10.3390/ijms19082231

Article

Comparative proteomics analysis of coregulation of CIPK14 and WHIRLY1/3 mediated leaf pale yellowing in *Arabidopsis*

Zhe Guan, Wanzhen Wang, Xingle Yu, Wenfang Lin, and Ying Miao*

Center for Molecular Cell and Systems Biology, Fujian Provincial Key Laboratory of Haixia Applied Plant Systems Biology, College of Life Sciences, Fujian Agriculture and Forestry University, 350002 Fuzhou, China. 1150539002@fafu.edu.cn (Z.G.); 1150539007@fafu.edu.cn (W.Z.W.); 17720802384@163.com (X.Y.); linwf@fafu.edu.cn (W.L.);

***Corresponding Author:** Ying MIAO, Email: ymiao@fafu.edu.cn; Tel/Fax: +86-591-8639-2987

Abstract: Leaf variegation pale yellowing is observed in the Calcineurin B-Like-Interacting Protein Kinase14 (CIPK14) overexpression line (*oeCIPK14*) and double knockout *WHIRLY1/WHIRLY3* (*why1/3*) lines of Arabidopsis, the distribution of WHIRLY1 (WHY1) protein between plastids and the nucleus are affected by the phosphorylation of WHY1 by CIPK14. To elucidate the coregulation of CIPK14 and WHIRLY1/WHIRLY3 mediated leaf pale yellowing, a differential proteomic analysis is conducted between the *oeCIPK14* variegated (*oeCIPK14-var*) line, *why1/3* variegated (*why1/3-var*) line and wild type (WT). More than 800 protein spots are distinguished on each gel, 67 differential abundance proteins (DAPs) are identified by matrix-assisted laser desorption ionization-time of flight/time of flight mass spectrometry (MALDI-TOF/TOF-MS), of which, 34 DAPs are in the *oeCIPK14-var*, 33 DAPs are in the *why1/3-var* compared to WT. Five overlapping proteins differentially change both in the *oeCIPK14-var* and in the *why1/3-var*. They are ATP-dependent Clp protease proteolytic subunit-related protein 3 (ClpR3), Ribulose bisphosphate carboxylase large chain (RBL), Beta-amylase 3 (BAM3), Ribosome-recycling factor (RRF), Ribulose bisphosphate carboxylase small chain (RBS). Bioinformatics analysis show that most of DAPs are involved in photosynthesis, defense and antioxidation pathway, protein metabolism, amino acid metabolism, energy metabolism, malate biosynthesis, lipid metabolism and transcription. Thus, the photosystem parameters are measured that the content of chlorophyll, the photochemical efficiency of PS Ⅱ (Fv/Fm), and electron transport rates (ETR) decrease in the *why1/3-var* and *oeCIPK14-var*, but the non-photochemical quenching (NPQ) increases. Both mutants show high sensitivity to strong light. Based on the annotation of DAPs from both *why1/3-var* and *oeCIPK14-var* lines, we conclude that CIPK14 phosphorylation mediated WHY1 deficiency in plastids is related to impairment of protein metabolism leading to chloroplast dysfunction.

Keywords: comparative proteomics analysis; CIPK14; WHIRLY1/WHIRLY3; protein metabolism

1. Introduction

Leaf senescence is a complex process that highly is regulated by genetic materials, and also is induced by internal (such as age and hormones) and external (including multiple biotic and abiotic stresses) factors [1]. Leaf senescence accompanies with the degradation of chlorophyll and various biomacromolecules in plant cells [1], the remobilization of nutrients to seeds and fruits during reproductive growth stage [2]. It has been reported that more than 20 transcription factor families are associated with senescence-regulation, such as NAC, WRKY, MYB, C2H2-type zinc finger and AP2/EREBP proteins families, many members of NAC and WRKY families have been reported to play a central role in leaf senescence regulatory network [3-7]. Among the WRKY families, *WRKY53* has been shown to act as a key regulator at early stage of leaf senescence in *Arabidopsis* [8], while

WHIRLY1 has been reported to repress the high expression of *WRKY53* by binding to the promoter of *WRKY53*, and delay the leaf senescence [9].

WHIRLY (WHY) family proteins are dually located in both the nucleus and organelles, and they perform numerous cellular functions in both locations [10, 11]. There are two WHY members (WHY1 and WHY2) in monocotyledonous plants, but three members (WHY1, WHY2 and WHY3) in dicotyledonous plants [12]. WHY: GFP fusion proteins fluorescence assay shows that the *Arabidopsis* WHY1 and WHY3 locate in chloroplasts, and WHY2 locates in mitochondria [10]. The intriguing feature of the dual location in plastids and the nucleus of WHY1 in the same cell has been demonstrated by immunogold-labelling assay in barley (*Hordeum vulgare*) [11]. The translocation of plastidial WHY1 protein from chloroplasts to the nucleus has been confirmed in the transplastomic tobacco plants which synthesized an HA-tagged version of WHY1 in plastids. The WHY1 protein is detected in the nucleus, where it changes the expression of target genes [13]. The characteristics of dual location and regulating nuclear gene transcription make WHY1 as an ideal candidate for plastid-to-nucleus retrograde signaling research.

WHY proteins are first discovered as nuclear transcriptional activator binding at elicitor response element in the promoter regions of pathogenesis-related genes in potato (*Solanum tuberosum*) and *Arabidopsis* [14, 15]. Later it is found that they are able to bind to various DNA sequences, including telomeres [16], a distal element upstream of a *kinesin* gene [17], the promoter region of the early senescence marker gene *WRKY53* in a development-dependent manner in *Arabidopsis* [9], and the promoter region of the senescence-associated gene *HvS40*, which was induced during natural and stress-related senescence in barley [18]. WHY1 is also proposed to bind to both ssDNA and RNA with a role in intron splicing in maize (*Zea mays*) chloroplasts [19], while in barley chloroplasts WHY1 is associated with intron-containing RNA [20].

Additionally, in *Arabidopsis*, plastid-located WHY1 and WHY3 both are identified as two novel plastid transcriptionally active chromosome proteins (pTACs) by mass spectrometry (MS) in transcriptionally active chromosomes of nucleoids [21]. At the same time, WHY3 and WHY1 both are found in the protein complex bound to the promoter of *kinesin* in *Arabidopsis* by pull down-MS assay [17]. While WHY3 is discovered as a redox-affected protein in the thiol-disulphide redox proteome of the chloroplast [22], WHY1 is proposed to involve in the perception of redox changes in the photosynthetic apparatus, the relocation of WHY1 from the chloroplasts to the nucleus may been initiated by the redox state of the photosynthetic electron transport chain [23]. A recent research indicates that WHY1 interacts with light-harvesting protein complex I (LHCA1) and affects the expression of genes encoding photosystem I (PS I) and light harvest complexes (LHCI) [24]. Although most double knockout *WHY1* and *WHY3* (*why1/3*) plants have no apparent phenotype, about 5% individuals show variegated phenotype which associated with the instability of plastid genome [25]. Furthermore, triple mutant *why1why3polIb-1* defective WHY1 and WHY3 and chloroplast DNA polymerase 1B (POLIB) exhibit a grievous variegated phenotype and higher plastid genome instability [26]. The *why1why3polIb-1* mutant shows lower photosynthetic efficiency and produces more reactive oxygen species (ROS) in chloroplast, the elevated ROS level is correlated with the intensive expression of oxidation-related nuclear genes [26]. In barley, *WHY1* RNAi knockdown mutants are shown to have more chlorophyll and less sucrose than the wild type [27]. Large numbers of genes encoding photosynthesis and protein synthesis proteins exhibit up-regulated expression in the *Hvwhy1* mutants [27]. These results suggest that plastid-located WHY proteins participate in plastid-to-nucleus retrograde signaling to maintain plastid function for environmental fluctuations response. Therefore, the dual location and dual function of WHY protein might have special traits in communication between two compartments in one cell.

The latest study has illuminated that the Calcineurin B-like-Interacting Protein Kinase14 (CIPK14) interacts with and phosphorylated WHY1, the phosphorylated WHY1 is imported to nucleus and enhances the binding affinity with the promoter of *WRKY53* [28]. *CIPK14* overexpression (*oeCIPK14*) plants show an increased nuclear isoform but decreased plastid isoform of WHY1, fascinatingly, among the *CIPK14* overexpression transgenic plants, about 5% individuals show variegated pale-green phenotype which is similar with *why1/3* and *why1why3polIb-1* [28]. Even more

intriguing, the variegated phenotype can be recovered partially by overexpression of plastid-located WHY1 [28].

This study focuses on comparable analysis of the phenotype and proteomic alteration between *why1/3* variegated (*why1/3-var*) lines and oe*CIPK14* variegated (*oeCIPK14-var*) lines for evaluating the relationship of CIPK14 and WHY1/WHY3 producing pale yellow leaf. The total proteins of wild type (WT), *why1/3-var* and *oeCIPK14-var* rosette leaves are separated by two-dimensional gel electrophoresis analysis (2-DE) and the differential expression proteins are identified by matrix-assisted laser desorption ionization-time of flight/time of flight mass spectrometry (MALDI-TOF/TOF-MS). The selected proteins are identified in transcriptional level by quantitative real-time PCR (qRT-PCR) and in protein level by western blot. The chlorophyll content and chlorophyll fluorescence kinetic curve are used to determine for photosynthetic performances analysis of the detail phenotype of different mutants.

2. Results

2.1. Proteomic analysis of why1/3-var and oeCIPK14-var mutants

Based on our previous reports, the dual localization and distribution of WHY1 protein between plastids and the nucleus were affected by WHY1 protein phosphorylation status mediated by CIPK14. The *CIPK14* overexpression transgenic plants, about 5% individual *oeCIPK14-var* showed variegated pale-green phenotype, which was similar with *why1/3-var* [28]. To evaluate the relationship of CIPK14 and WHY1/WHY3 producing pale yellow leaf on the protein level, proteomic analysis is conducted. The total proteins of rosette leaves of 4-week-old plants are separated by 2-DE, more than 800 protein spots are detected reproducibly on each gel for WT, *why1/3-var* and *oeCIPK14-var* lines. Total 67 differentially expressed protein spots show significant changing (fold>2, $p<0.05$) in the *why1/3-var* and *oeCIPK14-var* lines (Figure 1A-C). The differential expressed protein spots are analyzed by MALDI-TOF/TOF-MS, total 66 protein spots are identified successfully (identification rate: 99%), only one protein (spot 42) remains unknown. The identified proteins are listed in Table 1. Among them, 33 differentially expressed protein spots (spot 11, 14, 21, 30, 32, 35-62) are detected in the *why1/3-var* (Figure 1B), 34 differentially expressed protein spots (spot 1-34) are detected in the *oeCIPK14-var* (Figure 1C). Interestingly, only 5 overlapping proteins (spot 11, 14, 21, 30, 32) are discovered in both *why1/3-var* and *oeCIPK14-var*. These five proteins are proposed to intimately associate with the CIPK14 mediating functions of WHY proteins.

In order to evaluate the quality of 2-DE differentially display proteins, two light-dependent reaction complex related proteins are selected to do immunodetection by using consumable antibodies against the ATP synthase subunit alpha (atp A) and the photosystem Ⅱ (PS Ⅱ) complex proteins PSBR (Figure 1D). While an antibody against atp A didn't work, PSBR is barely detectable in the *oeCIPK14-var* that is in agreement with the changes of protein abundance observed by 2-DE (Figure 1D). We further directly detect the RBL and RBS amount by coomassie bright blue R250 staining (Figure 1D), it clearly shows that both RBL and RBS decrease in the *why1/3-var* and *oeCIPK14-var* lines, which is in consistent with the changes of protein abundance observed by 2-DE. Furthermore, two antibodies against RBL and RBS (kindly provided by Krupinska lab) are used to perform western blot. The results show consistently in the *why1/3-var* and *oeCIPL14-var* lines that the proteins RBL and RBS both are down-regulated in the *oeCIPK14-var* and slightly decreases in the *why1/3-var* plants compared to wild-type plants (Figure1D). It confirms the MS data reliable.

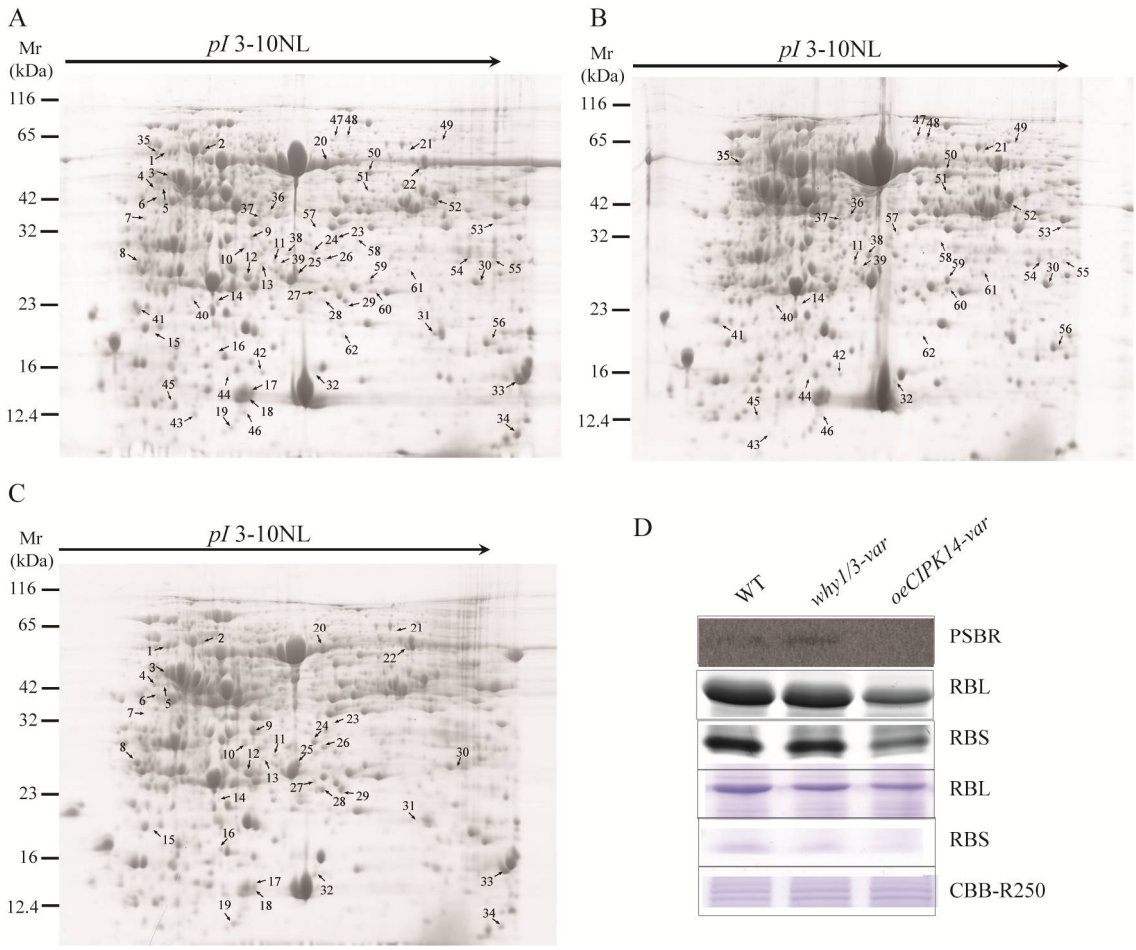

Figure 1. 2-DE and immunoblot analysis of total proteins extracted from rosette leaves of WT and two variegated mutants. (A-C) Representative 2-DE gel images of WT (A), *why1/3-var* (B), and *oeCIPK14-var (C).* An equal amount (1.5 mg) of total proteins is loaded on each IPG strips (3-10 NL).The spot numbers indicated proteins that showed significant changes between WT and two variegated mutants. (D) The changing of protein abundance selected from 2-DE are confirmed by western blot and CBB R250 staining. The immunoblot analysis is performed using antibodies against RBL, RBS, and PSBR. CBB R250 staining shows RBL and EBS protein amount and the same amount of loading proteins.

2.2. Functional classification of differentially expressed proteins

Based on Uniprot database (http://www.uniprot.org/) and the description from the literatures, the function of 65 proteins have been annotated. These proteins are categorized into 8 groups based on their biochemical functions as shown in Table 1. The majority of the proteins are photosynthesis-associated proteins, followed by defense and antioxidation proteins, protein metabolism and amino acid metabolism, energy metabolism, malate biosynthesis, lipid metabolism and transcription related proteins (Table 1 and Figure 2). Comparative analysis of differentially expression proteins between *why1/3-var*/WT and *oeCIPK14-var*/WT are shown in Figure 2A and 2B, respectively. The five overlapping proteins between *why1/3-var*/WT and *oeCIPK14-var*/WT are ATP-dependent Clp protease proteolytic subunit-related protein 3 (ClpR3), Ribulose bisphosphate carboxylase large chain (RBL), Beta-amylase 3 (BAM3), Ribosome-recycling factor (RRF), Ribulose bisphosphate carboxylase small chain (RBS) (Figure 2C).

Peer-reviewed version available at Int. J. Mol. Sci. 2018, 19, 2231; doi:10.3390/ijms19082231

161

162 ***Table 1*** *Differential proteins identified by MALDI-TOF/TOF-MS of why1/3-var and CIPK14-var*

Spot no[a]	Protein name[b]	Accession no[c]	Mascot score	Matched peptides	Theor MW (kDa)/pI[d]	Cov%[e]	Subcellular Loc[f]
Light reaction							
1	Fe-S cluster assembly factor HCF101	HF101_ARATH	371	13	57.728/5.91	20%	plastid
2	RCA	F4IVZ7_ARATH	499	18	48.469/7.55	34%	chloroplast
3	ATP synthase subunit alpha	ATPA_ARATH	927	32	55.294/5.19	50%	plastid
4	Magnesium-chelatase subunit ChlI-2	CHLI2_ARATH	365	23	46.069/5.36	44%	chloroplast
12	Chlorophyll a-b binding protein CP26	CB5_ARATH	213	12	30.183/6	35%	plastid
26	Magnesium protoporphyrin IX methyltransferase	CHLM_ARATH	653	23	33.775/7.68	53%	chloroplast
28	PsbP domain-containing protein 4	PPD4_ARATH	122	8	28.484/7.02	33%	plastid
33	Oxygen-evolving enhancer protein 3-2	PSBQ2_ARATH	464	16	24.628/9.72	59%	plastid
34	PSBR	A0A178WGP6_ARATH	112	7	9.77/10.1	39%	plastid
35	TROL	A0A178V0X3_ARATH	444	21	54.448/5.09	29%	chloroplast
Calvin cycle							
5	Phosphoglycerate kinase 1	PGKH1_ARATH	642	24	50.081/5.91	37%	chloroplast
6	Sedoheptulose-1,7-bisphosphatase	S17P_ARATH	354	18	42.388/6.17	28%	chloroplast
14	Ribulose bisphosphate carboxylase large chain (Fragment)	A0A142I795_ARATH	292	12	51.833/6.17	9%	chloroplast
17	Ribulose bisphosphate carboxylase small chain	A0A178UL15_ARATH	326	14	20.33/7.59	45%	chloroplast
18	Ribulose bisphosphate carboxylase small chain 1A	RBS1A_ARATH	369	15	20.203/7.59	45%	chloroplast
23	Ribulose bisphosphate carboxylase large chain (Fragment)	A0A142I795_ARATH	292	12	51.833/6.17	18%	plastid
27	Ribulose bisphosphate carboxylase large chain	RBL_ARATH	740	31	52.922/5.88	42%	chloroplast
32	Ribulose bisphosphate carboxylase small chain	A0A178UL15_ARATH	326	14	20.33/7.59	45%	chloroplast

Peer-reviewed version available at Int. J. Mol. Sci. 2018, 19, 2231; doi:10.3390/ijms19082231

40	Ribulose bisphosphate carboxylase large chain (Fragment)	A0A142I795_ARATH	292	12	51.833/6.17	26%	chloroplast
43	Ribulose bisphosphate carboxylase small chain 1A	RBS1A_ARATH	362	13	20.203/7.79	49%	chloroplast
45	Ribulose bisphosphate carboxylase small chain 1B	RBS1B_ARATH	348	14	18.506/8.22	53%	chloroplast
59	Beta carbonic anhydrase 1	BCA1_ARATH	307	15	37.426/5.74	48%	plastid/ cytomembrane
Defense and antioxidation							
7	Glucan endo-1,3-beta-glucosidase, acidic isoform	E13A_ARATH	568	16	37.316/4.85	33%	secretion
9	Thiamine thiazole synthase	THI4_ARATH	183	10	36.641/5.82	28%	plastid
10	SAPX	A0A178V0Q5_ARATH	524	24	40.446/8.31	47%	chloroplast
16	Glycine-rich RNA-binding protein 7	RBG7_ARATH	167	9	16.88/5.85	51%	cytoplasm/nucleus
20	Glutathione S-transferase F6	GSTF6_ARATH	355	15	23.471/5.8	49%	cytoplasm
24	V-type proton ATPase subunit E1	VATE1_ARATH	328	30	26.044/6.04	75%	vacuole
25	L-ascorbate peroxidase 1	F4HU93_ARATH	389	16	27.503/5.85	52%	cytoplasm
37	Pyridoxal 5'-phosphate synthase subunit PDX1.1	PDX11_ARATH	423	23	32.841/5.75	37%	cytoplasm
38	Thioredoxin-like protein CDSP32	CDSP_ARATH	371	20	33.663/8.65	35%	chloroplast
44	GRP7	A0A178VQY8_ARATH	315	9	16.937/5.85	37%	cytoplasm/nucleus
46	V-type proton ATPase subunit G1	VATG1_ARATH	304	10	12.389/5.77	70%	vacuole
51	Formate dehydrogenase	FDH_ARATH	354	18	42.383/7.12	36%	chloroplast/mitochondria
52	12-oxophytodienoate reductase 3	OPR3_ARATH	782	24	42.664/7.71	54%	peroxysome
54	Thylakoid lumenal 29 kDa protein	TL29_ARATH	475	24	37.911/8.59	53%	plastid
55	Remorin	REMO_ARATH	427	26	20.955/8.63	65%	plasmalemma
57	VIPP1	A0A178W0D3_ARATH	412	23	28.895/5.9	67%	plastid
60	Glutathione S-transferase F7	GSTF7_ARATH	552	18	23.583/6.14	52%	cytoplasm
61	Peptide methionine sulfoxide reductase A4	MSRA4_ARATH	236	12	38.626/8.96	26%	plastid
Amino acid metabolism							
22	Serine hydroxymethyltransferase 4	GLYC4_ARATH	504	22	51.685/6.8	46%	cytoplasm
48	Asparagine synthetase [glutamine-hydrolyzing] 2	ASNS2_ARATH	235	18	64.989/6.01	27%	cytoplasm/plasmodesmata

Peer-reviewed version available at Int. J. Mol. Sci. 2018, 19, 2231; doi:10.3390/ijms19082231

50	Glutamate-glyoxylate aminotransferase 1	GGT1_ARATH	478	20	53.267/6.49	37%	peroxysome
58	Acetylglutamate kinase	NAGK_ARATH	424	14	36.572/9.04	36%	plastid
Proteometabolism							
11	ATP-dependent Clp protease proteolytic subunit-related protein 3	CLPR3_ARATH	597	23	36.284/8.64	41%	chloroplast
13	Proteasome subunit alpha type-6-A	PSA6A_ARATH	926	25	27.277/5.6	58%	cytoplasm/ nucleus
15	30S ribosomal protein S6 alpha	RR6_ARATH	119	8	22.746/5.92	26%	plastid
19	CPN10	O80504_ARATH	567	10	15.04/8.75	45%	chloroplast
29	Proteasome subunit beta type-2-B	PSB2B_ARATH	715	22	21.97/6.21	70%	cytoplasm/nucleus
30	Ribosome-recycling factor	RRFC_ARATH	497	18	30.403/9.46	44%	plastid
31	Peptidyl-prolyl cis-trans isomerase CYP18-3	CP18C_ARATH	307	11	18.361/7.68	34%	cytoplasm
39	Proteasome subunit alpha type-6-B	PSA6B_ARATH	312	19	27.333/5.75	56%	cytoplasm/nucleus
56	Peptidyl-prolyl cis-trans isomerase CYP19-1	CP19A_ARATH	406	14	18.48/8.65	43%	cytoplasm
62	Nascent polypeptide-associated complex subunit beta	A0A178W6R8_ARATH	332	14	16.935/5.50	45%	cytoplasm/nucleus
Energy metabolism							
21	Beta-amylase 3	BAM3_ARATH	510	24	61.314/6.59	41%	chloroplast
Malate biosynthesis							
36	Malate dehydrogenase	MDHP_ARATH	334	12	42.379/8.66	23%	chloroplast
47	NADP-dependent malic enzyme 2	MAOP2_ARATH	323	19	64.372/6.01	25%	cytoplasm
49	L-galactono-1,4-lactone dehydrogenase	GLDH_ARATH	759	35	68.513/8.7	38%	mitochondria
Lipid metabolism							
53	GDSL esterase/lipase At1g29670	GDL15_ARATH	841	19	39.847/8.85	44%	secretion
Transcription							
8	RNA-binding protein CP29B	CP29B_ARATH	602	16	30.699/5.06	52%	plastid
Unknow function							

41	At1g13930/F16A14.27	Q9XI93_ARATH	310	14	16.154/4.82	87%	chloroplast/plasmalemma
42	Kinesin-like calmodulin-binding protein	KCBP_ARATH	54	35	143.359/6.69	21%	cytoplasm

a. Numbering corresponds to 2-DE gel in Figure 1A-C.
b. Database accession of the identified proteins in uniprot (http://www.uniprot.org/).
c. Molecular mass and pI theoretical.
d. Percentage of predicted protein sequence with match sequence.
e. Subcellular localization of the identified protein base on uniprot and previous literatures.

168

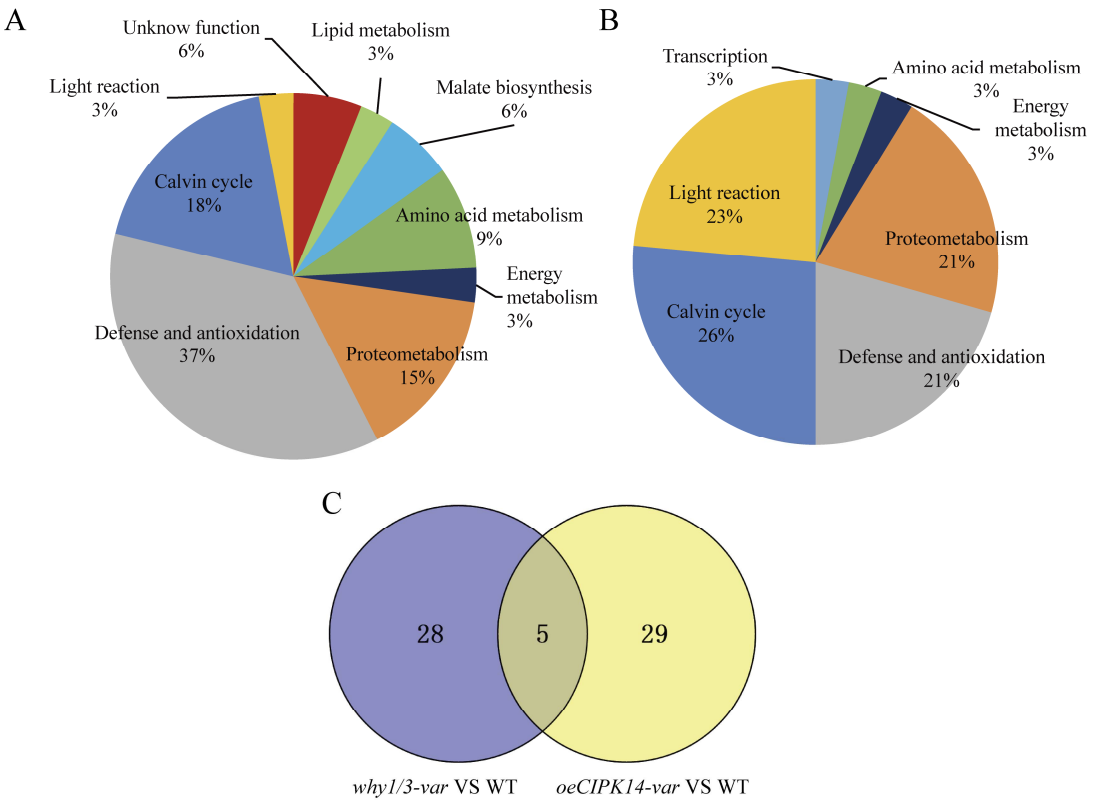

169

170 **F**igure 2. Functional classifications of the differentially expressed proteins identified in *why1/3-var* and
171 *oeCIPK14-var* compared with WT. (**A**) Functional classifications of the differentially expressed
172 proteins between *why1/3-var* and WT; (**B**) Functional classifications of the differentially expressed
173 proteins between *oeCIPK14-var* and WT; (**C**) The Venn diagram analysis between *why1/3-var* and
174 *oeCIPK14-var* compared with WT. The Venn diagram is completed by the online tool
175 (http://bioinfogp.cnb.csic.es/tools/venny/index.html).

176 *2.3. Hierarchical clustering analysis of differentially expressed proteins*

177 To acquire information of identified proteins, hierarchical clustering analysis is performed in the
178 proteins which appeared on the same branch with the similar expression pattern (Figure 3). It is
179 shown that there are 4 clusters for these proteins. The majority of proteins in the first and second
180 clusters are up-regulated in the *why1/3-var* and *oeCIPK14-var* lines, respectively, mainly containing
181 defense and antioxidation related proteins (spot 9, 10, 25, 37, 38, 52, 54, 57, 61), amino acid and protein
182 metabolism related proteins (spot 11, 19, 22, 29, 30, 39, 48, 50), photosynthesis-associated proteins
183 (spot 1, 3, 4, 6, 12, 26, 28, 32, 35) and energy metabolism related proteins (spot 21, 36, 47, 51). Most of
184 proteins in the third and fourth clusters show down-regulated in the *why1/3-var* and *oeCIPK14-var*
185 lines, respectively. Among them, some of the key enzymes of Calvin cycle (spot 2, 5, 6, 14, 17, 18, 23,
186 27, 40, 43, 45) belong to the two branches, suggesting that the fixation rates of CO_2 decrease in the
187 *why1/3-var* and *oeCIPK14-var* variegated lines. We also find that other proteins are down-regulated in
188 the *why1/3-var* and *oeCIPK14-var*, which are involved in light-reaction, defense and antioxidation
189 mechanisms, amino acid metabolism, proteins metabolism and so on.

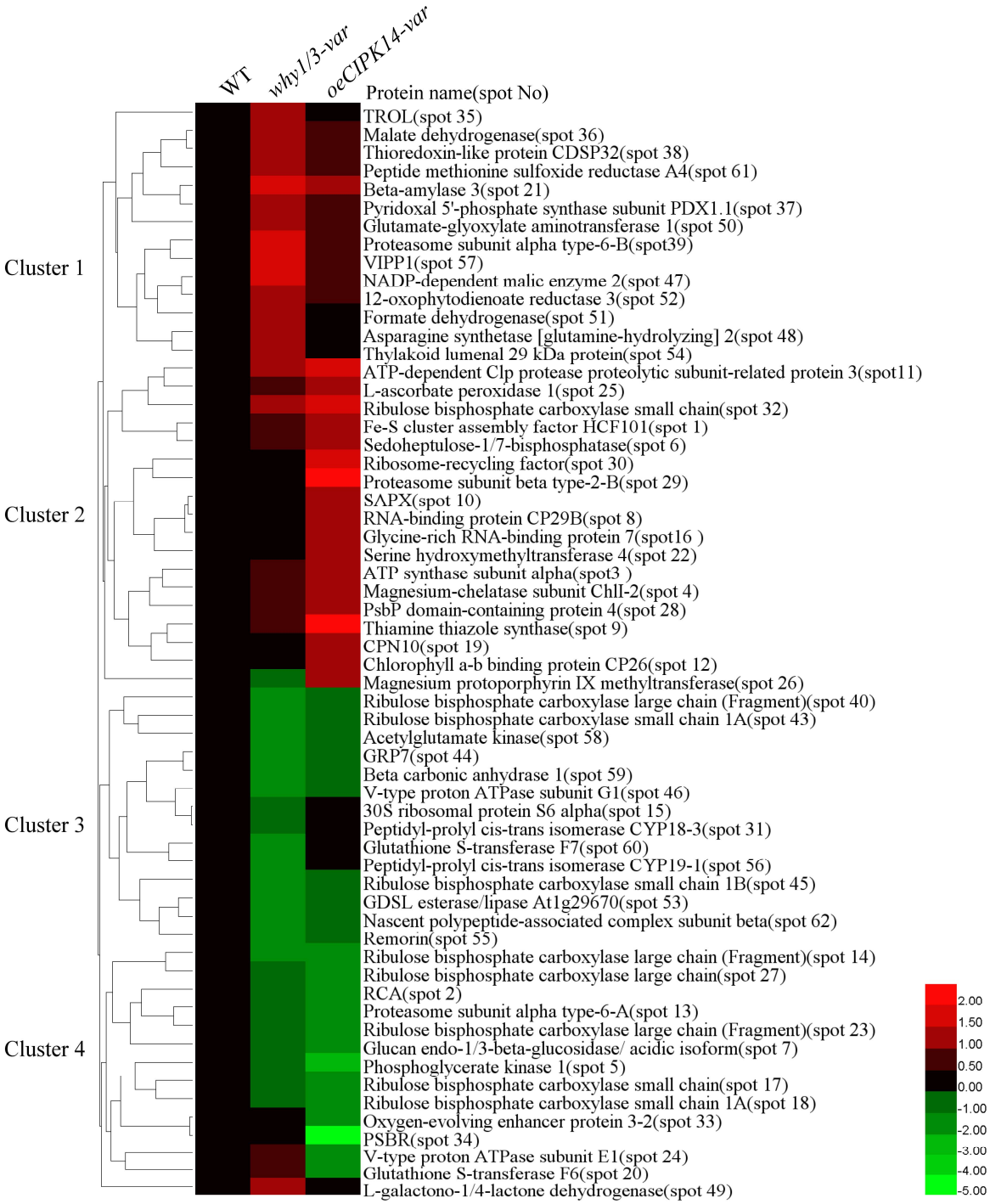

Figure 3. Hierarchical cluster analysis of the differentially expressed proteins of *why1/3-var* and *oeCIPK14-var* compared with WT. The three columns represent protein expression changings in the (A) WT, (B) *why1/3-var*, (C) *oeCIPK14-var*, respectively. The rows represent individual proteins identified in the *why1/3-var* and *oeCIPK14-var* lines, the up-regulated or down-regulated proteins are indicated in red or green. The heat map used log2 of fold changes of protein abundance between WT and *why1/3-var* and *oeCIPK14-var* mutants.

2.4. Transcriptional level analysis of the encoding genes of differentially expressed proteins

To investigate the correlation between protein and transcript levels. The transcript levels of the encoding genes of differentially expressed proteins are analyzed by quantitative real-time PCR (qRT-PCR). 26 genes are determined in the WT, *why1/3-var*, and overexpressing WHY1 (*oeWHY1)* lines; and 27 genes are determined in the WT, *oeCIPK14-var*, and knockout *CIPK14 (cipk14)* lines,

respectively. The transcript levels of WHY1, WHY3 and CIPK14 firstly detect in the WHY and CIPK14 mutants (Figure 4). As show in Figure 4, the expression level of *WHIRLY1* is barely detectable in the *why1/3-var* but significant accumulation in the *oeWHY1* (Figure 4A). The expression level of *WHIRLY3* is lower in the *why1/3-var* compared with WT (Figure 4B). The expression level of *CIPK14* is barely detectable in the *cipk14* while it shows significant up-regulation in the *oeCIPK14-var* (Figure 4C).

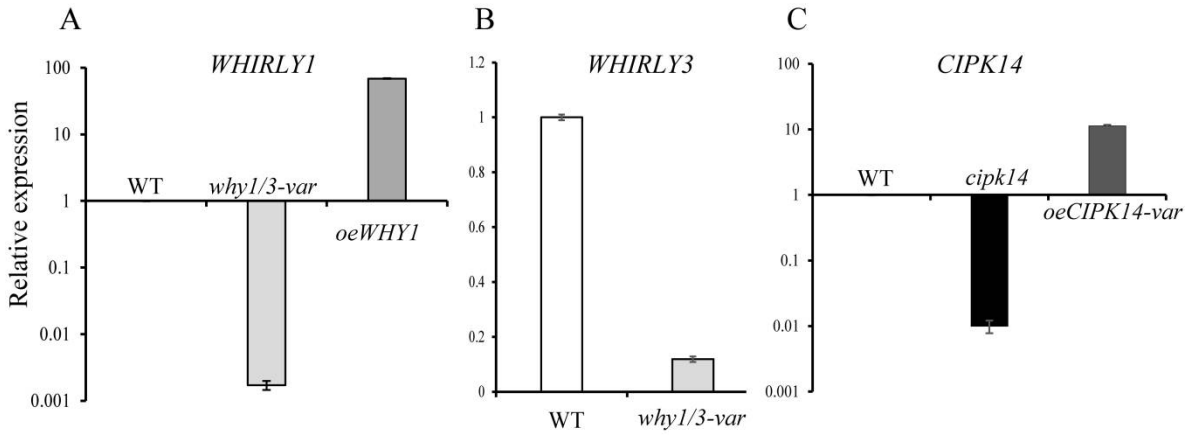

Figure 4. The transcript levels of *WHIRLY1*, *WHIRLY3* and *CIPK14* in the used lines. (A) The level of expression of *WHIRLY1* in the WT, *why1/3-var* and *oeWHY1*; (B) The level of expression of *WHIRLY3* in the WT and *why1/3-var*; (C) The level of expression of *CIPK14* in the WT, *cipk14* and *oeCIPK14-var*.

We further analyze the transcript levels of the encoding genes of differentially expressed proteins. Relative protein abundance of WT and *why1/3-var* is represented by percent volume on up panel (a1 and b1) of Figure 5A and 5B panel, the relative expression levels of the encoding genes of differentially expressed proteins in the *why1/3-var* and *oeWHY1* compared WT are shown in the Figure 5A-a2 and Figure 5B-b2 panel, respectively. The encoding genes of differentially expressed proteins in the *oeCIPK14-var* are analyzed in the WT, *cipk14* and *oeCIPK14-var*. Relative protein abundance of WT and *oeCIPK14-var* is represented by percent volume on the up panel (c1 and d1) of Figure 5C and 5D panel, the relative expression levels of the encoding genes of differentially expressed proteins in the *oeCIPK14-var* and *cipk14* compared WT are shown in the Figure 5C-c2 and Figure 5D-d2 panel, respectively. The quantitative RT-PCR results of all candidate genes show that the transcript level of 11 out of 26 genes is altered in the *why1/3-var* or *oeWHY1*, among them the transcriptional patterns of 5 out of 26 genes are consistent with the protein expression patterns (Figure 5A-a2), whereas the rest 21 genes show inconsistency in the *why1/3-var* (Figure 5B-b2), however, most of gene expression changings in the *why1/3-var* are recovered in the *oeWHY1* except for spot 21, spot 39, and spot 44. It suggests that WHY1 is not enough to fully rescue the alteration of transcript level of genes in the *why1/3-var*. The transcript level of 13 out of 27 gene expression is changed in the *oeCIPK14-var* or *cipk14*, among them the mRNA levels of 9 out of the 27 genes change in parallel with protein levels (Figure 5C-c2), whereas the rest 18 genes show inconsistency in the *oeCIPK14-var* (Figure 4D-d2). Unexpectedly, only a few gene expression levels are changed in the *cipk14* line, no any gene expression is rescued. This discrepancy between the mRNA and protein levels may be caused by the different half-lives of protein and mRNA, or post-transcriptional or post-translational process and modification.

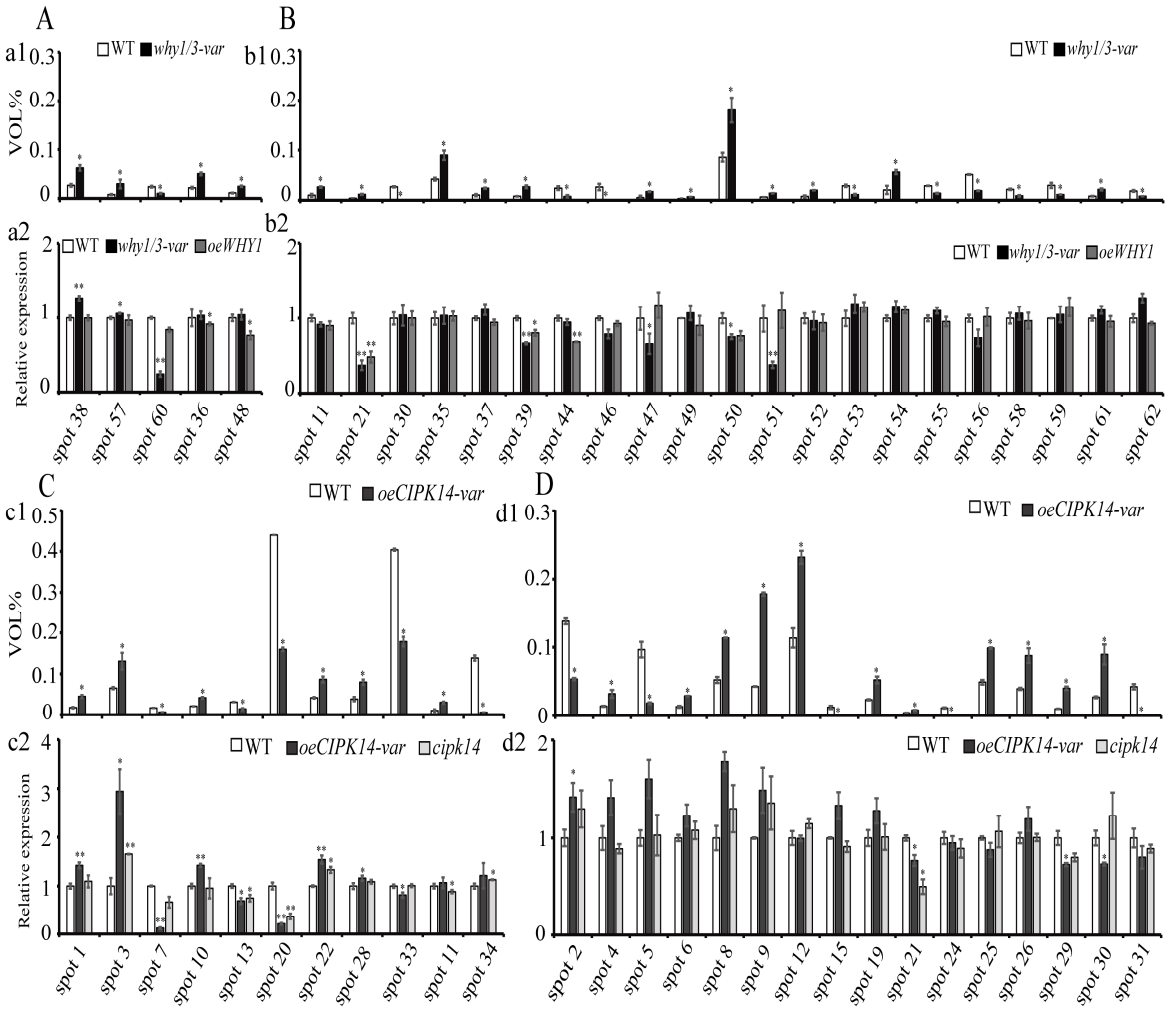

Figure 5 Comparison of changes in the protein and mRNA levels for selected protein spots. The relative protein abundance is represented by percent volume. (**A**) The mRNA levels change in parallel with protein levels in the *why1/3-var* lines; (**a1**) The relative protein abundance of protein spots in the WT and *why1/3-var*; (**a2**) The relative expression levels of the corresponding genes in (a1) are analyzed in the WT, *why1/3-var,* and *oeWHY1*; (**B**) The mRNA levels change independently in the *why1/3-var* lines; (**b1**) The relative protein abundance of protein spots in the WT and *why1/3-var;* (**b2**) The relative expression levels of the corresponding genes (b1) are analyzed in the WT, *why1/3-var*, and *oeWHY1;* (**C**) The mRNA levels change in parallel with protein levels in the *oeCIPK14-var* lines; (**c1**) The relative protein abundance of protein spots in the WT and *oeCIPK14-var*; (**c2**) The relative expression level of the corresponding genes in (c1) are analyzed in the WT, *oeCIPK14-var*, and *cipk14*; (**D**) The mRNA levels change independently in the *oeCIPK14-var* lines; (**d1**) The relative protein abundance of protein spots in the WT and *oeCIPK14-var*; (**d2**) The relative expression of the corresponding genes in (**d1**) are analyzed in the WT, *oeCIPK14-var*, and *cipk14.*

The relative expression level of the gene is normalized to *GAPC2*, with the WT as 1. The error bars indicated standard error of three biological replications and three technique replicates. Asterisk indicate significant differences (*P<0.05 and **P<0.01) based on Student's t-test analyzed by Graphpad prism6 software.

2.5. Effects of why1/3-var and oeCIPK14-var on photosynthetic performance

According to above protein annotations, the majority of the differentially expressed proteins are photosynthesis-associated proteins. In order to address the relationship of these protein function and phenotype of pale green leaf appeared in the *why1/3-var* and *oeCIPK14-var* lines, the chlorophyll contents and photosynthetic fluorescence parameters of 4-week-old plants of *WHY* and *CIPK14*

mutants are measured to determine the photosynthetic performance. Consistent with the pale-green phenotype, the chlorophyll content is lower in the *oeCIPK14-var* plants than wild-type, whereas it remains unaltered in the *why1/3-var* (Figure 6A). Interestingly, the chlorophyll content slightly increases in the *oeWHY1* and *cipk14* plants (Figure 6A). The maximum photochemical efficiency of photosystem II (Fv/Fm) significantly decreases in the *why1/3-var* and *oeCIPK14-var* plants (Figure 6B). The electron transport rates (ETR) in the *why1/3-var* and *oeCIPK14-var* are only about 70% and 45% of the WT, respectively (Figure 6C). The nonphotochemical quenching of photosystem II fluorescence (NPQ) displays an increase in the *why1/3-var* and *oeCIPK14-var* (Figure 6D), indicating that the two variegated mutants have a lower photosynthetic capacity. It is consistence with plants under high light condition.

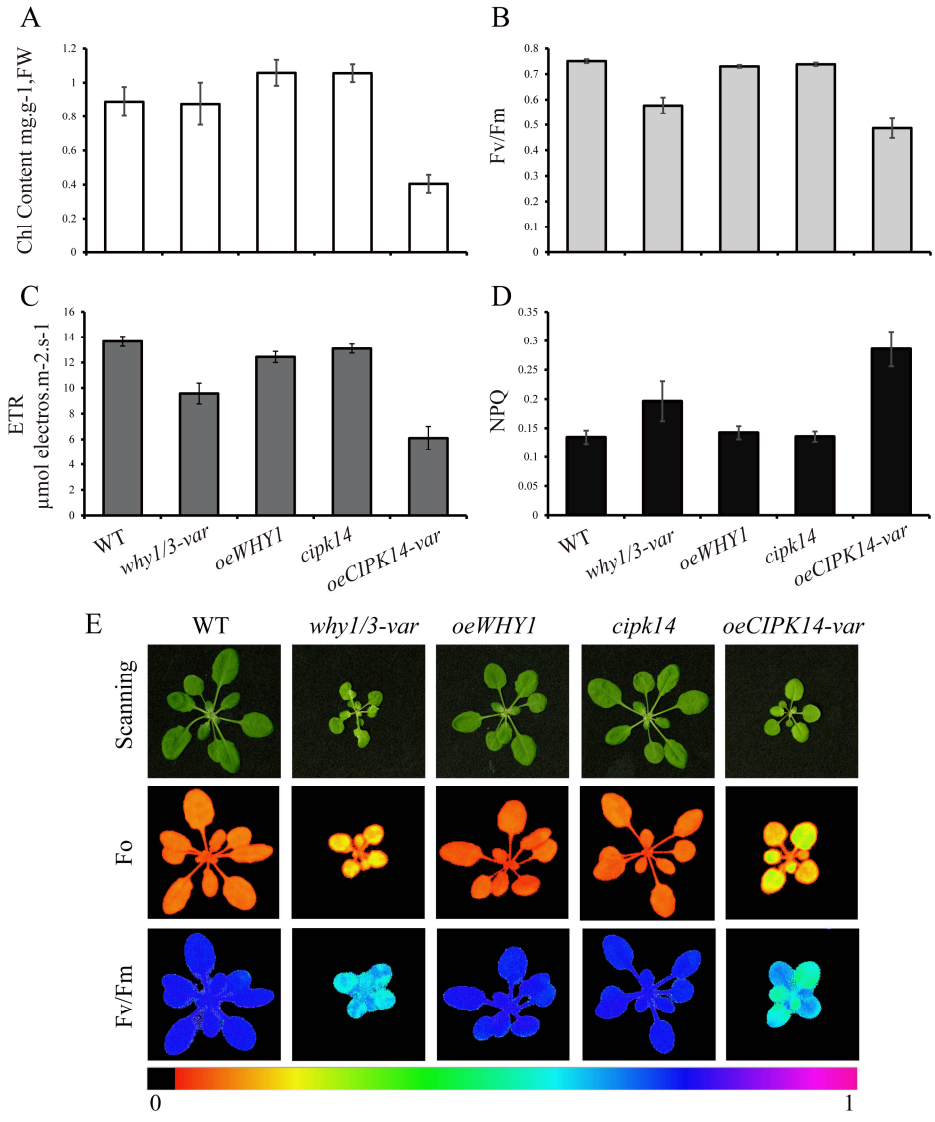

Figure 6 The photosynthetic performance analysis of WHY and CIPK14 mutants. (A) Total chlorophyll content. (B) The maximum photochemical efficiency of photosystem II (Fv/Fm). (C) The nonphotochemical quenching of photosystem II fluorescence (NPQ). (D)The electron transport rate (ETR).The error bars indicate the standard error of nine independent measurements. (E) The fluorescence images of the whole plants of WHY and CIPK14 mutants. The fluorescence images are taken by Image-PAM using the plants after 30 minutes dark-adapted.

The fluorescence images of the whole plant of different genotype are taken by using Image-PAM (Pulse-Amplitude Modulation) measuring system, as showed in Figure 6E. The *why1/3-var* and *oeCIPK14-var* plants display the smaller size and variegated phenotype as described previously [25, 28]. While the *oeWHY1* and *cipk14* plants are almost indistinguishable from the wild type, however,

the dark fluorescence yield (F0) of the two variegated lines are higher, but the Fv/Fm decreases remarkably in the *why1/3-var* and *oeCIPK14-var* lines..

Taken together, in the *why1/3-var* and *oeCIPK14-var* plants higher F0, lower Fv/Fm, and lower ETR, higher NPQ may lead to excessive excitation energy production, which may enhance the level of ROS production. The unbalance of energy may further result in the variation of redox state of the photosynthetic electron transport chain, then trigger the relocation of WHY1 from the chloroplasts to the nucleus and transmitted the signals.

3. Discussion

Leaf pale yellowing phenotype normally appears in plastid dysfunction plants such as plastid ribosome defect plants, chlorophyll syntheses abnormal plants or plastid RNA processing abnormal plants. As expected, in this study, most of differential display proteins in the *why1/3-var*/WT *oeCIPK14-var*/WT are related plastid dysfunction, such as photosynthesis, amino acids and protein metabolism, or defense and antioxidation.

3.1 Protein involved in light-dependent reaction of photosynthesis

The dual-located protein WHY1 has suggested as an ideal candidate for plastid-to-nucleus retrograde signaling factor [23]. In chloroplast, the WHY1 is located at the boundary between thylakoids and the nucleoids and therefore the WHY1 protein is proposed to link the operation of the photosynthetic electron transport chain to gene expression [23]. WHY3 has found as cofactors of WHY1 playing a function in the plastid genome stability [25], and activators in the nuclear *kinesin* gene expression [17]. In our study, the results of functional classification and immunoblot analysis reveal that the 7 light reaction related proteins including Fe-S cluster assembly factor HCF101 (HCF101, spot 1), Magnesium-chelatase subunit ChlI-2 (ChlI-2, spot 4), atpA (spot 3), Chlorophyll a-b binding protein CP26 (CP26, spot 12), PsbP domain-containing protein 4 (PPD4, spot 28), TROL (spot 35) and cyt f exhibit more abundance in the *why1/3-var* and *oeCIPK14-var* plants. The PPD4 and CP26 are the components of PSII [29, 30]. CP26 is known as an antenna protein which required for the formation of PSII supercomplexes and the energy transition from trimeric light-harvesting complex II (LHCII) to the reaction center of PSII [31]. The Cyt b6f complex modulating the electrons transferring from PSII to PSI are performed by the quinone pool and plastocyanin [28]. The increase in abundance of cyt f may accelerate the ETR that are lower in the *why1/3-var* and *oeCIPK14-var* plants. The HCF101 has been shown to serve as a chloroplast scaffold protein for the assembly and transferring of [4Fe-4S] clusters which are essential for the accumulation of the core complex PSI and the soluble ferredoxin-thioredoxin reductases [32]. The ATP synthase is responsible for ATP production, the up-regulated of atpA is observed in our proteomic data. As expected, we also find that the TROL (spot 35) protein is required for tethering of FNR and sustaining efficient linear electron flow (LEF) [33]. The TROL knockout mutant displays lower ETR and increases NPQ, it further confirms our former result which the *why1* line showed low TROL protein [24]. Consistent with the pale-green phenotype of two variegated lines, the enzyme of chlorophyll biosynthesis ChlI-2 shows up-regulated and it catalyzes the first committed step toward chlorophyll synthesis, accompanying Mg^{2+} inserts into protoporphyrin IX and produces Mg-protoporphyrin IX [31]. In addition, another key enzyme of chlorophyll biosynthesis magnesium protoporphyrin IX methyltransferase (spot 26) also exhibits up-regulated in the *oeCIPK14-var* [35], it suggests that plants may increase the accumulation of chlorophyll and transport to the two PSs for the synthesis of LHC complex, then maintain the efficiency of electron transfer and alleviate the stress of excessive energy. Thylakoid lumenal 29 kDa protein (TL29, spot 54) is targeted in the thylakoid lumen of chloroplasts [36], which was identified as a homology of ascorbate peroxidase associated with PS II [37], it shows more abundance in the *why1/3-var* and *oeCIPK14-var*.

3.2 Protein involved in Calvin cycle

Several essential proteins of the Calvin cycle are down-regulated expression in the *why1/3-var* and *oeCIPK14-var*, including ribulose bisphosphate carboxylase large chain (RbcL, spot 14, 23, 27, 40), ribulose bisphosphate carboxylase small chain (RbcS, spot 17, 18, 43, 45), ribulose-1,5-bisphosphate carboxylase/oxygenase (Rubisco) activase (RCA, spot 2), Phosphoglycerate kinase (PGK, spot 5). It is well known that Rubisco, a complex of eight RbcL and eight RbcS subunits containing eight catalytic sites, is the most abundant protein in the earth, utilized by autotrophic organisms to transform CO2 into organic compounds via the Calvin-Benson cycle [38]. Rubisco catalyzes the rate-limiting step of photosynthetic carbon reduction for CO_2 assimilation [38]. In this study, except for spot 32, all the other RbcL and RbcS are decreased. The activity of Rubisco is inhibited by RCA, which it can release the ribulose-1, 5-bisphosphate (RuBP) from the active sites of Rubisco by using the energy from ATP hydrolysis by increasing ratios of ADP to ATP in *Arabidopsis* [39], so that CO_2 can activate the enzyme [39], indicating that the redox states of photosynthetic electron transport chain are changed, and the production of ATP are inhibited. PGK can catalyze the conversion of 3-phosphoglycerate to 1, 3-bisphosphoglycerate which is a substrate for the synthesis of glyceraldehyde-3-phosphate (G3P) in Calvin-Benson cycle, G3P serves as a substrate for the synthesis of other carbohydrates [40], Carbonic Anhydrase 1(CA, spot 59) is located in the chloroplast and catalyzes the interconversion of H_2O and CO_2 into HCO_3- which involves in CO_2-dependent stomatal closing [41]. The expression of CA is also decreased in the *why1/3-var* and *oeCIPK14-var* lines, implying that the photosynthetic efficiency is changed.

3.3 Protein associated with defense and antioxidation

The results of photosynthetic performance analysis suggest that *why1/3-var* and *oeCIPK14-var* lines show lower photosynthetic electron transport efficiencies. However, several defense and antioxidation related proteins (spot 9, 10, 16, 25, 37, 38, 54, and 61) are up-regulated in the *why1/3-var* and *oeCIPK14-var* for ROS scavenging. Among them, thiamine thiazole synthase (THI, spot 9) and Pyridoxal 5-phosphate synthase subunit PDX1.1 (PDX, spot 37) are reported that they up-regulate expression under oxidative stress [42]. THI (spot 9) is involved in biosynthesis of the thiamine (vitamin B1) precursor thiazole [43]; The PDX (spot 37) catalyzes the formation of pyridoxal 5'-phosphate that is phosphorylated derivatives of VB6, which can act as a coenzyme for numerous metabolic enzymes and has been identified as a potent antioxidant [44, 45]. The identified protein SAPX (spot 10) and L-ascorbate peroxidase APX1 (spot 10 and spot 25) have been proposed to reduce the generation of ROS and enhance the tolerance in oxidative stress [46, 47]. Additional proteins: the thioredoxin-like protein CDSP32 (spot 38) has been reported as a thioredoxin and is involved in plastid responses to oxidative stress [48]; the enzyme peptide methionine sulfoxide reductase (PMSR) (spot 61) can catalyze the reduction of Met sulfoxides back to Met [49], it has been shown to repair oxidative damaged proteins in chloroplasts [48]; the VIPP1 (spot 57) is an essential component for thylakoid biogenesis in chloroplasts [50], which it is up-regulated expression for the membrane maintenance, when the envelope membrane integrity of chloroplast was disturbed[51]. Two members of glutathione S-transferase (GST) family proteins like glutathione S-transferase F6 (spot 20, GSTF6) and Glutathione S-transferase F7 (spot 60, GSTF7) are identified in this study. GSTF6 (spot 20) is up-regulated in the *why1/3-var*, but down-regulated in the *oeCIPK14-var*. GST F7 is decreased in the *why1/3-var*. Taken together, it indicates that WHY1/WHY3 or CIPK14 both are involved in ROS balance case. The *why1/3* or *oeCIPK14* affecting the excessive excitation energy may trigger the accumulation of ROS in chloroplasts;

3.4 Proteins related to protein metabolism

Intriguingly, in the present study, several identified protein spots are involved in protein metabolism. Among them, five spots (spot 11, 19, 29, 30 and 39) show an increased abundance in the *why1/3-var* and *oeCIPK14-var*. For example, the ATP-dependent Clp protease is one of plastid protease that plays an essential role in chloroplast development and maintains [52, 53]. ATP-dependent Clp protease proteolytic subunit-related protein 3 (spot 11) is up-regulated in the *why1/3-var* and *oeCIPK14-var* indicating chloroplast dysfunction. In general, selective proteolysis in plants is largely

mediated by the ubiquitin (Ub)/26S proteasome system [54], the abnormal polypeptides are marked by the covalent attachment of Ub, are degraded by the 26S proteasome [55], the 26S proteasome is composed of two subparticles, the 20S core protease and the 18S regulatory particle [55], 20S core protease subunit beta type-2-B (spot 29) and proteasome subunit alpha type-6-B (spot 39) [55] and protease subunit alpha type-6-A (spot 13) all show down-regulated in the *why1/3-var* and *oeCIPK14-var*; Ribosome-recycling factor (spot 30, RRF) located in the chloroplast [56], increases in the *oeCIPK14-var* lines, which is essential for embryogenesis and chloroplast biogenesis, and supposes to be involved in translation of chloroplast proteins [56]; The chaperonin CNP10 (spot 19) also is shown to be localized to the chloroplasts [57], and up-regulated in the *oeCIPK14-var*, which is essential proteins involved in cellular protein folding [57]. In addition, our data show that RNA-binding protein CP29B (spot 8) up-regulates in the *oeCIPK14-var*, which is a kind of a chloroplast RNA binding proteins and may involve in processing of chloroplast RNA [58]. It demonstrates that CIPK14 mediating plastid WHY1/WHY3 protein might be involved in plastid protein metabolism including protein translation, synthesis, and proteolysis (Figure 7).

Although the transcription levels of the encoding genes of these proteins are not fully confirmed their altering trend, it can be explained that in one hand the discrepancy between mRNA and protein levels may be caused by the different half-lives of protein and mRNA, or post-transcriptional or post-translational process and modification. In fact, several identified protein spots are involved in protein metabolism, post-transcriptional or post-translational process and modification. In other hand, it seems that the alteration of the transcriptional levels in the *why1/3-var* and *oeCIPK14-var* could not rescue in the *oeWHY1* or *cipk14* mutants. It has been reported that in maize, *why1* plants with pale yellowing phenotype was supposed to be related to impairment of RNA processing [19, 20], however in *Arabidopsis* only double mutated *why1/3* showed pale yellowing phenotype [25]. It hints that WHY1 protein in monocotyledon plant evolutionary shares functions of both WHY1 and WHY3 in dicotyledonous *Arabidopsis*. It will be addressed by genetically rescued experiment in future. It is not such unexpected that *cipk14* plant cannot be recused the leaf pale yellowing phenotype of *oeCIPK14-var* and the gene expression pattern of *oeCIPK14-var*. Actually, CIPK14 mainly acts as a kinase, phosphorylates WHY1 and pushes WHY1 enter in the nucleus, mostly showing staygreen phenotype[28], and only 5% plants showing pale yellowing. The leaf pale yellowing of *oeCIPK14-var* resulted from WHY1/WHY3 deficiency can be rescued by overexpressing plastid isoform WHY1 [28]. In fact, in this study, five proteins (ClpR3, RBL, RBS, RRF and BAM3) show an alternative abundance in the *why1/3-var* and *oeCIPK14-var*, interestingly, their mutants all have been reported showing similar leaf yellowing and small rosette phenotypes [53, 56, 59]. Their speculating mechanism of action connecting with CIPK14 and WHIRLY protein mediated leaf pale yellowing in protein metabolism will be detailed addressed in coming future.

4. Materials and Methods

4.1. Plant Materials and Growth Conditions

Plants of *Arabidopsis thaliana* Columbia ecotype and the mutants are cultivated in the vermiculite matrix after vernalization. Plants are grown in a controlled climatic chamber at 13/11 h light/dark cycle with a periodic temperature 22℃/18℃, a light intensity of 60 μmol·m^{-2}s^{-1}, and a relative humidity of 65%. The rosette leaves of the plants are collected at 4 weeks after germination for each genotype. The samples are frozen in liquid nitrogen prior and stored at -80℃ before used. Three biological replicates are used for each experiment.

T-DNA insertion lines SALK_023713 (*why1*) for WHY1 and SALK_009699 (*cipk14*) for CIPK14 are provided by NASC. Seeds of *WHY1* and *WHY3* double mutant (*why1/3*) are kindly provided by Prof. Normand Brisson, Department of Biochemistry, Montreal University, Montreal, Canada. Overexpression of *WHY1* (*oeWHY1*) and *CIPK14* (*oeCIPK14*) lines are prepared from the former work [28].

4.2. Chlorophyll Content Measurement and Photosynthetic Parameters Analysis

Colored threads are used for rosette leaves labelling after their emergence as previously described [8]. The weight of leaf 5 from 12 independent 4-week-old plants are measured, and each leaf with one milliliter 95% ethanol (v/v) in the 1.5 milliliter (mL) Eppendorf tube. Pigments are extracted after incubating 48 hours in dark. Absorbance of extracts is measured at 470, 649, and 665 nm by the Flexstation 3 Microplate Reader (Molecular Devices, USA), and the total chlorophyll content is determined according the method as described [60].

Chlorophyll fluorescence is measured and chlorophyll fluorescence image is taken using an Imaging-PAM-Maxi (Walz, Germany) as described by Shao [60]. The leaf 5 from 4-week-old plants are selected for measurement after 30 minutes adaptation of darkness, the minimal fluorescence yield (Fo) is measured at a low light intensity and the maximal fluorescence yield (Fm) is measured under saturation pulse, then all of leaves are exposed to a light intensity of 54 $\mu mol \cdot m^{-2}s^{-1}$ photosynthetically active radiation (PAR), the kinetic curves are gained according the instruction of the instrument. The maximum photochemical efficiency of photosystem II (Fv/Fm), the nonphotochemical quenching of photosystem II fluorescence (NPQ), the electron transport rate (ETR) are calculated by the control software. The chlorophyll fluorescence images of whole plant are taken after 30 minutes adaptation of darkness. Through one saturation pulse, the values of Fo and Fv/Fm are calculated and formed fluorescence image by Imaging-PAM-Maxi (Walz, Germany).

4.3. Protein Extraction and 2-DE Analysis

The total proteins of rosette leaf are extracted by the phenol method [62]. In brief, approximately 3 g material is ground with liquid nitrogen, then is suspended in 12 mL ice-cold extraction buffer contains 50 mM PBS (PH 7.8) , 5mM EDTA, 2% (v/v) β-mercaptoethanol, 0.5% (v/v) NP-40, 1 mM Phenylmethane -sulfonyl fluoride (PMSF), 1% (w/v) polyvinylpolypyrrolidone (PVPP) on ice and vortexed for 5 min. An equal volume of ice-cold Tris-saturation phenol (pH 8.0) adds to suspension and vortexes for 10 min. The phenol phase is collected after centrifugation (4 ℃, 15 min, 16000 g), and proteins are precipitated over night with five volumes 0.1 M methanol/ammonium acetate at -20 ℃. The protein pellets are collected after centrifugation (4 ℃, 15 min, 16000 g) and rinsed three times in ice-cold acetone/13mM dithiothreitol (DTT). Between each wash, the proteins are incubated for 1 hour at -20℃. After centrifugation (4 ℃, 15 min, 16000 g), the supernatant is discarded carefully and the protein pellets are air-dried.

The protein pellets are dissolved in sample lysis buffer (7 M urea, 2 M thiourea, 4% CHAPS, 65 mM DTT, 2% IPG Buffer pH 3-10 NL), and protein concentrations are determined by Bradford method [63]. A total of 1.5 milligram (mg) protein are loaded onto an IPG Strip (24 cm, 3-10 NL) and rehydrated 12 h at 25 ℃. Ettan IPGphor system (GE Healthcare, American) is employed for Isoelectric focusing (IEF) in a program manner: 30 V (0.5 h), 100 V (1 h) , 200 V (1 h) , 500 V (3 h) , 1 kV (1 h) , 10 kV (2 h, gradient) and finally 10 kV up to 60000 Vhs. Then the strips are equilibrated for 15 min in equilibration buffer I contains 50 mM Tris–HCl (pH 8.8), 6 M urea, 30% (v/v) glycerol, 2% (w/v) SDS, 1% DTT, and in equilibration buffer II contains 50 mM Tris–HCl (pH 8.8), 6 M urea, 30% (v/v) glycerol, 2% (w/v) SDS, 2.5% iodoacetamide for 15 min with gentle shaking. After equilibration, the strips are transferred onto 12.5% SDS-PAGE and performed with an Ettan DALT-six System (GE Healthcare, American) at 10 mA per gel for 1 h and then 15 mA per gel overnight. After electrophoresis, the 2-DE gels are stained by the Coomassie Brilliant Blue R250 (CBB R250). Three independent biological replicates are used for each genotype.

4.4. Data analysis in-gel protein digestion and protein identification

Gels are scanned at 600 dpi resolution with a scanner (EPSON Expression 11000XT, Japan), and the images are quantitative analyzed by ImageMaster™ 2D Platinum 7.0 software (GE Healthcare, American). The differential protein spots are in-gel digestion and identification according to the methods as described. In shortly, the protein spots are excised from the CCB R250 stained gels and subjected to in-gel trypsin digestion for 12 h at 37 ℃. Peptides are extracted twice within 50% ACN/0.1% TFA, then the extracts dried completely by a vacuum centrifuge. Peptide mixtures are dissolved in 0.1% TFA, 0.8 μl of peptide solution is mixed with 0.4 μl of matrix*α*-cyano-4-

hydroxycinnamic acid in 30% ACN/0.1% TFA before spotting on the target plate. An AB SCIEX MALDI TOF-TOFTM 5800 Analyzer (AB SCIEX, Foster City, CA) equipped with a neodymium: yttrium-aluminum-garnet laser (laser wavelength was 349 nm) is employed for acquiring peptide mass fingerprint (PMF). All automatic data analysis and database searching are conducted using GPS Explorer TM software (version 3.6, AB SCIEX) running a mascot search algorithm (v2.3, Matrix Science, London, UK) for protein identification. Proteins with protein score confidence intervals (C.I.) above 95% (protein score >61) are considered confident identifications. The identified proteins are then matched to specific processes or functions by searching Uniprot.

4.5. RNA extraction, reverse transcription and qRT-PCR analysis

Total RNA is extracted from the 4-week-old rosette leaves of Arabidopsis using the Trizol Reagents (TransZol up, TRANSGEN BIOTECH, China) according to the protocol of manufacturer. First-strand cDNA is synthesized using the cDNA Synthesis SuperMix with gDNA Removal (TRANSGEN BIOTECH, China) according to the manufacturer's instructions. Specific oligo nucleotide primers are designed by http://quantprime.mpimp-golm.mpg.de, and synthesized by Sangon Biotech (Shanghai, China). Quantitative real-time PCR using the Ultra SYBR Mixture (CWBIO, China) according to the manufacturer's instructions, and is performed by a Lightcycler ® 96(Roche, Switzerland). The *GAPC2* is used as an internal standard and relative gene expression are analyzed using $2^{-\Delta\Delta C\,(T)}$ Method. The primer pairs are shown in supplemental table S1.

4.6. Immunological Analyses

Proteins are extracted from rosette leaves according to the phenol method [62]. Equal amounts of proteins are determined by Bradford method [63]. Proteins are separated on 12.5% polyacrylamide gels [65], transferred to PVDF membranes by semi-dry electroblotting, and immunodetected according the protocols as described [24]. Primary antibodies directed toward the CYTF, PSBP, PSBR and LHCA1 were purchased from Agrisera (Sweden).

5. Conclusions

We concluded that in the *why1/3-var* or *oeCIPK14-var* lines most of proteins are involved in photosynthesis, amino acids and protein metabolism, or defense and antioxidation (Figure 7). They are related to photosynthesis and insufficiencies in energy supply. The co-regulation of CIPK14 phosphorylation mediated WHIRLY1/WHIRLY3 deficiency in plastids are speculated that they might be controlled by mechanism of amino acids and plastid protein metabolism at the posttranscriptional level. The detail mechanism will be addressed in future.

Preprints (www.preprints.org) | NOT PEER-REVIEWED | Posted: 6 July 2018 doi:10.20944/preprints201807.0111.v1

Peer-reviewed version available at Int. J. Mol. Sci. 2018, 19, 2231; doi:10.3390/ijms19082231

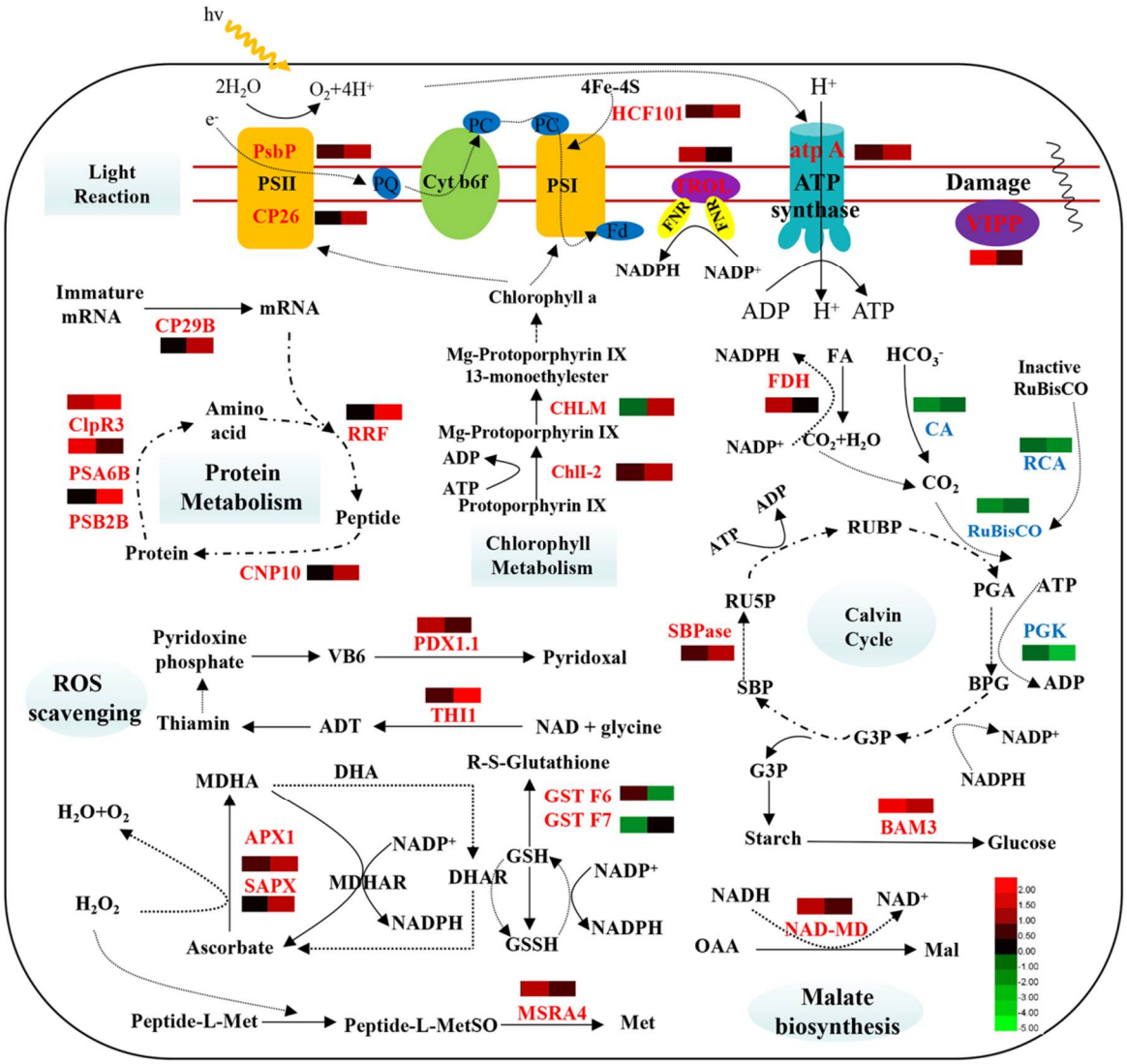

why1/3-var oe*CIPK14-var*

Figure 7. Summary of CIPK14 or/and WHIRLY1/3 mediated pathways in chloroplasts, including light reaction, chlorophyll metabolism, ROS scavenging, malate biosynthesis, calvin cycle, and protein metabolism.

Abbreviations: ADP, adenosine diphosphate; ADT, adenosine diphosphate 5-(2-hydroxyethyl)-4-methylthiazole-2-carboxylic acid; APX1, L-ascorbate peroxidase 1; ATP, adenosine triphosphate; ATPA, ATP synthase alpha subunit; BAM3, beta-amylase 3; BPG, 1,3-diphosphoglycerate; CA, carbonic anhydrase; ChlI-2, magnesium-chelatase subunit ChlI-2; CHLM, magnesium protoporphyrin IX methyltransferase; CLPR3, ATP-dependent Clp protease proteolytic subunit-related protein 3; CNP10, 10 kDa chaperonin; CP26, chlorophyll a-b binding protein CP26; CP29B, RNA-binding protein CP29B; Cyt b6f, cytochrome b6f; DHAR, dehydroascorbate reductase; FA, formate; Fd, ferredoxin; FDH, formate dehydrogenase; FNR, ferredoxin-NADP (H) oxidoreductase; G3P, glyceraldehydes-3-phosphate; GSH, reduced glutathione; GSSH, oxidized glutathione; GST, glutathione S-transferase; HCF101, Fe-S cluster assembly factor HCF101; Mal, malate; MD, malate dehydrogenase; MDHA, monodehydroascorbate; MDHAR, MDHA reductase; Met, methionine; MetSO, methionine sulfoxide; MSRA4, peptide methionine sulfoxide reductase A4; NADP+/NADPH, nicotinamide adenine dinucleotide phosphate; NAD+/NADH, nicotinamide adenine dinucleotide; OAA, oxaloacetic acid; PC, plastocyanin; PDX1.1, pyridoxal 5'-phosphate synthase subunit PDX1.1; PGA, 3-phosphoglycerate; PGK, phosphoglycerate kinase; PQ, plastoquinone; PSI, photosystem I; PSII, photosystem II; PSA6B, proteasome subunit alpha type-6-B; PSB2B, proteasome subunit beta type-2-B; PsbP, PsbP domain-containing protein 4; RCA, ribulose-1,5-bisphosphate

carboxylase/oxygenase activase; RRF, ribosome-recycling factor; Ru5P, ribulose-5-phosphate; RuBisCO, ribulose-1,5-bisphosphate carboxylase/oxygenase; THI, thiamine thiazole synthase; TROL, thylakoid rhodanese-like protein; SBP, sedoheptulose-1,7-bisphosphate; SBPase, sedoheptulose-1,7-bisphosphatase; SAPX, stromal ascorbate peroxidase; VB6, vitamin B6; VIPP1, vesicle-inducing protein in plastids.

Acknowledgements: We acknowledge Prof. Normand Brisson (Department of Biochemistry, Montreal University, Montreal, Canada) kindly provided *why1/3* double mutants. T-DNA insertion line *SALK_009699* (*cipk14*) for CIPK14 were provided by NASC. This work was supported by a grant of NSFC (31470383, 31770318) and a grant of NSF of Fujian Province Key Project (2015N0019).

Author's contribution: Y.M. designed the research; Z.G., W.W. and X. Y. performed all experiments. W.L. helped to analyze the data; Z.G and Y.M. analyzed data and wrote the paper.

Conflicts of Interest: The authors declare no conflict of interest.

References

1. Lim, P. O.; Kim, H. J.; Nam, H. G., Leaf senescence. *Annual Review of Plant Biology* **2007,** 58, 115-36.
2. Pottier, M.; Masclaux-Daubresse, C.; Yoshimoto, K.; Thomine, S., Autophagy as a possible mechanism for micronutrient remobilization from leaves to seeds. *Frontiers in Plant Science* **2014,** 5, 11.
3. Balazadeh, S.; Riano-Pachon, D. M.; Mueller-Roeber, B., Transcription factors regulating leaf senescence in Arabidopsis thaliana. *Plant Biology* **2008,** 10 Suppl 1, 63-75.
4. Balazadeh, S.; Siddiqui, H.; Allu, A. D.; Matallana-Ramirez, L. P.; Caldana, C.; Mehrnia, M.; Zanor, M. I.; Kohler, B.; Mueller-Roeber, B., A gene regulatory network controlled by the NAC transcription factor ANAC092/AtNAC2/ORE1 during salt-promoted senescence. *The Plant Journal* **2010,** 62, (2), 250-64.
5. Balazadeh, S.; Kwasniewski, M.; Caldana, C.; Mehrnia, M.; Zanor, M. I.; Xue, G. P.; Mueller-Roeber, B., ORS1, an H(2)O(2)-responsive NAC transcription factor, controls senescence in Arabidopsis thaliana. *Molecular Plant* **2011,** 4, (2), 346-60.
6. Zentgraf, U.; Laun, T.; Miao, Y., The complex regulation of WRKY53 during leaf senescence of Arabidopsis thaliana. *European Journal of Cell Biology* **2010,** 89, (2-3), 133-7.
7. Zhou, X.; Jiang, Y.; Yu, D., WRKY22 transcription factor mediates dark-induced leaf senescence in Arabidopsis. *Molecules and Cells* **2011,** 31, (4), 303-13.
8. Hinderhofer, K.; Zentgraf, U., Identification of a transcription factor specifically expressed at the onset of leaf senescence. *Planta* **2001,** 213, (3), 469-73.
9. Miao, Y.; Jiang, J.; Ren, Y.; Zhao, Z., The single-stranded DNA-binding protein WHIRLY1 represses WRKY53 expression and delays leaf senescence in a developmental stage-dependent manner in Arabidopsis. *Plant Physiology* **2013,** 163, (2), 746-56.
10. Krause, K.; Kilbienski, I.; Mulisch, M.; Rodiger, A.; Schafer, A.; Krupinska, K., DNA-binding proteins of the Whirly family in Arabidopsis thaliana are targeted to the organelles. *FEBS letters* **2005,** 579, (17), 3707-12.
11. Grabowski, E.; Miao, Y.; Mulisch, M.; Krupinska, K., Single-stranded DNA-binding protein Whirly1 in barley leaves is located in plastids and the nucleus of the same cell. *Plant Physiology* **2008,** 147, (4), 1800-4.
12. Desveaux, D.; Marechal, A.; Brisson, N., Whirly transcription factors: defense gene regulation and beyond. *Trends in Plant Science* **2005,** 10, (2), 95-102.

13. Isemer, R.; Mulisch, M.; Schafer, A.; Kirchner, S.; Koop, H. U.; Krupinska, K., Recombinant Whirly1 translocates from transplastomic chloroplasts to the nucleus. *FEBS letters* **2012,** 586, (1), 85-8.
14. Desveaux, D.; Despres, C.; Joyeux, A.; Subramaniam, R.; Brisson, N., PBF-2 is a novel single-stranded DNA binding factor implicated in PR-10a gene activation in potato. *The Plant Cell* **2000,** 12, (8), 1477-89.
15. Desveaux, D.; Subramaniam, R.; Despres, C.; Mess, J. N.; Levesque, C.; Fobert, P. R.; Dangl, J. L.; Brisson, N., A "Whirly" transcription factor is required for salicylic acid-dependent disease resistance in Arabidopsis. *Developmental Cell* **2004,** 6, (2), 229-40.
16. Yoo, H. H.; Kwon, C.; Lee, M. M.; Chung, I. K., Single-stranded DNA binding factor AtWHY1 modulates telomere length homeostasis in Arabidopsis. *The Plant Journal* **2007,** 49, (3), 442-51.
17. Xiong, J. Y.; Lai, C. X.; Qu, Z.; Yang, X. Y.; Qin, X. H.; Liu, G. Q., Recruitment of AtWHY1 and AtWHY3 by a distal element upstream of the kinesin gene AtKP1 to mediate transcriptional repression. *Plant Molecular Biology* **2009,** 71, (4-5), 437-49.
18. Krupinska, K.; Dahnhardt, D.; Fischer-Kilbienski, I.; Kucharewicz, W.; Scharrenberg, C.; Trosch, M.; Buck, F., Identification of WHIRLY1 as a Factor Binding to the Promoter of the Stress- and Senescence-Associated Gene HvS40. *J Plant Growth Regulator* **2014,** 33, (1), 91-105.
19. Prikryl, J.; Watkins, K. P.; Friso, G.; van Wijk, K. J.; Barkan, A., A member of the Whirly family is a multifunctional RNA- and DNA-binding protein that is essential for chloroplast biogenesis. *Nucleic Acids Research* **2008,** 36, (16), 5152-65.
20. Melonek, J.; Mulisch, M.; Schmitz-Linneweber, C.; Grabowski, E.; Hensel, G.; Krupinska, K., Whirly1 in chloroplasts associates with intron containing RNAs and rarely co-localizes with nucleoids. *Planta* **2010,** 232, (2), 471-81.
21. Pfalz, J.; Liere, K.; Kandlbinder, A.; Dietz, K. J.; Oelmuller, R., pTAC2, -6, and -12 are components of the transcriptionally active plastid chromosome that are required for plastid gene expression. *The Plant Cell* **2006,** 18, (1), 176-97.
22. Stroher, E.; Dietz, K. J., The dynamic thiol-disulphide redox proteome of the Arabidopsis thaliana chloroplast as revealed by differential electrophoretic mobility. *Physiologia Plantarum* **2008,** 133, (3), 566-83.
23. Foyer, C. H.; Karpinska, B.; Krupinska, K., The functions of WHIRLY1 and REDOX-RESPONSIVE TRANSCRIPTION FACTOR 1 in cross tolerance responses in plants: a hypothesis. *Philosophical transactions of the Royal Society of London. Series B, Biological Sciences* **2014,** 369, (1640), 20130226.
24. Huang, D.; Lin, W.; Deng, B.; Ren, Y.; Miao, Y., Dual-Located WHIRLY1 Interacting with LHCA1 Alters Photochemical Activities of Photosystem I and Is Involved in Light Adaptation in Arabidopsis. *International Journal of Molecular Sciences* **2017,** 18, (11).
25. Marechal, A.; Parent, J. S.; Veronneau-Lafortune, F.; Joyeux, A.; Lang, B. F.; Brisson, N., Whirly proteins maintain plastid genome stability in Arabidopsis. *Proceedings of the National Academy of Sciences of the United States of America* **2009,** 106, (34), 14693-8.
26. Lepage, E.; Zampini, E.; Brisson, N., Plastid genome instability leads to reactive oxygen species production and plastid-to-nucleus retrograde signaling in Arabidopsis. *Plant Physiology* **2013,** 163, (2), 867-81.
27. Comadira, G.; Rasool, B.; Kaprinska, B.; Garcia, B. M.; Morris, J.; Verrall, S. R.; Bayer, M.; Hedley, P. E.; Hancock, R. D.; Foyer, C. H., WHIRLY1 Functions in the Control of Responses to Nitrogen Deficiency But Not Aphid Infestation in Barley. *Plant Physiology* **2015,** 168, (3), 1140-51.
28. Ren, Y.; Li, Y.; Jiang, Y.; Wu, B.; Miao, Y., Phosphorylation of WHIRLY1 by CIPK14 Shifts Its Localization and Dual Functions in Arabidopsis. *Molecular Plant* **2017,** 10, (5), 749-763.

29. Balsera, M.; Arellano, J. B.; Gutierrez, J. R.; Heredia, P.; Revuelta, J. L.; De Las Rivas, J., Structural analysis of the PsbQ protein of photosystem II by Fourier transform infrared and circular dichroic spectroscopy and by bioinformatic methods. *Biochemistry* **2003,** 42, (4), 1000-7.

30. Jansson, S., A guide to the Lhc genes and their relatives in Arabidopsis. *Trends in Plant Science* **1999,** 4, (6), 236-240.

31. de Bianchi, S.; Dall'Osto, L.; Tognon, G.; Morosinotto, T.; Bassi, R., Minor antenna proteins CP24 and CP26 affect the interactions between photosystem II subunits and the electron transport rate in grana membranes of Arabidopsis. *The Plant Cell* **2008,** 20, (4), 1012-28.

32. Schwenkert, S.; Netz, D. J.; Frazzon, J.; Pierik, A. J.; Bill, E.; Gross, J.; Lill, R.; Meurer, J., Chloroplast HCF101 is a scaffold protein for [4Fe-4S] cluster assembly. *The Biochemical Journal* **2009,** 425, (1), 207-14.

33. Juric, S.; Hazler-Pilepic, K.; Tomasic, A.; Lepedus, H.; Jelicic, B.; Puthiyaveetil, S.; Bionda, T.; Vojta, L.; Allen, J. F.; Schleiff, E.; Fulgosi, H., Tethering of ferredoxin:NADP+ oxidoreductase to thylakoid membranes is mediated by novel chloroplast protein TROL. *The Plant Journal* **2009,** 60, (5), 783-94.

34. Kobayashi, K.; Mochizuki, N.; Yoshimura, N.; Motohashi, K.; Hisabori, T.; Masuda, T., Functional analysis of Arabidopsis thaliana isoforms of the Mg-chelatase CHLI subunit. *Photochemical & photobiological sciences : Official journal of the European Photochemistry Association and the European Society for Photobiology* **2008,** 7, (10), 1188-95.

35. Pontier, D.; Albrieux, C.; Joyard, J.; Lagrange, T.; Block, M. A., Knock-out of the magnesium protoporphyrin IX methyltransferase gene in Arabidopsis. Effects on chloroplast development and on chloroplast-to-nucleus signaling. *The Journal of Biological Chemistry* **2007,** 282, (4), 2297-304.

36. Kieselbach, T.; Hagman; Andersson, B.; Schroder, W. P., The thylakoid lumen of chloroplasts. Isolation and characterization. *The Journal of Biological Chemistry* **1998,** 273, (12), 6710-6.

37. Granlund, I.; Storm, P.; Schubert, M.; Garcia-Cerdan, J. G.; Funk, C.; Schroder, W. P., The TL29 protein is lumen located, associated with PSII and not an ascorbate peroxidase. *Plant & Cell Physiology* **2009,** 50, (11), 1898-910.

38. Andersson, I.; Backlund, A., Structure and function of Rubisco. *Plant Physiology and Biochemistry* **2008,** 46, (3), 275-91.

39. Portis, A. R., Jr., Rubisco activase - Rubisco's catalytic chaperone. *Photosynthesis Research* **2003,** 75, (1), 11-27.

40. Rosa-Tellez, S.; Anoman, A. D.; Flores-Tornero, M.; Toujani, W.; Alseek, S.; Fernie, A. R.; Nebauer, S. G.; Munoz-Bertomeu, J.; Segura, J.; Ros, R., Phosphoglycerate Kinases Are Co-Regulated to Adjust Metabolism and to Optimize Growth. *Plant Physiology* **2018,** 176, (2), 1182-1198.

41. Hu, H.; Boisson-Dernier, A.; Israelsson-Nordstrom, M.; Bohmer, M.; Xue, S.; Ries, A.; Godoski, J.; Kuhn, J. M.; Schroeder, J. I., Carbonic anhydrases are upstream regulators of CO2-controlled stomatal movements in guard cells. *Nature Cell Biology* **2010,** 12, (1), 87-93; sup pp 1-18.

42. Tunc-Ozdemir, M.; Miller, G.; Song, L.; Kim, J.; Sodek, A.; Koussevitzky, S.; Misra, A. N.; Mittler, R.; Shintani, D., Thiamin confers enhanced tolerance to oxidative stress in Arabidopsis. *Plant Physiology* **2009,** 151, (1), 421-32.

43. Belanger, F. C.; Leustek, T.; Chu, B.; Kriz, A. L., Evidence for the thiamine biosynthetic pathway in higher-plant plastids and its developmental regulation. *Plant Molecular Biology* **1995,** 29, (4), 809-21.

44. Tambasco-Studart, M.; Titiz, O.; Raschle, T.; Forster, G.; Amrhein, N.; Fitzpatrick, T. B., Vitamin B6 biosynthesis in higher plants. *Proceedings of the National Academy of Sciences of the United States of America* **2005,** 102, (38), 13687-92.

45. Bilski, P.; Li, M. Y.; Ehrenshaft, M.; Daub, M. E.; Chignell, C. F., Vitamin B6 (pyridoxine) and its derivatives are efficient singlet oxygen quenchers and potential fungal antioxidants. *Photochemistry and Photobiology* **2000,** 71, (2), 129-34.

46. Maruta, T.; Tanouchi, A.; Tamoi, M.; Yabuta, Y.; Yoshimura, K.; Ishikawa, T.; Shigeoka, S., Arabidopsis chloroplastic ascorbate peroxidase isoenzymes play a dual role in photoprotection and gene regulation under photooxidative stress. *Plant & Cell Physiology* **2010,** 51, (2), 190-200.

47. Davletova, S.; Rizhsky, L.; Liang, H.; Shengqiang, Z.; Oliver, D. J.; Coutu, J.; Shulaev, V.; Schlauch, K.; Mittler, R., Cytosolic ascorbate peroxidase 1 is a central component of the reactive oxygen gene network of Arabidopsis. *The Plant Cell* **2005,** 17, (1), 268-81.

48. Rey, P.; Cuine, S.; Eymery, F.; Garin, J.; Court, M.; Jacquot, J. P.; Rouhier, N.; Broin, M., Analysis of the proteins targeted by CDSP32, a plastidic thioredoxin participating in oxidative stress responses. *The Plant Journal* **2005,** 41, (1), 31-42.

49. Brot, N.; Weissbach, L.; Werth, J.; Weissbach, H., Enzymatic reduction of protein-bound methionine sulfoxide. *Proceedings of the National Academy of Sciences of the United States of America* **1981,** 78, (4), 2155-8.

50. Romero, H. M.; Berlett, B. S.; Jensen, P. J.; Pell, E. J.; Tien, M., Investigations into the role of the plastidial peptide methionine sulfoxide reductase in response to oxidative stress in Arabidopsis. *Plant Physiology* **2004,** 136, (3), 3784-94.

51. Zhang, L.; Kato, Y.; Otters, S.; Vothknecht, U. C.; Sakamoto, W., Essential role of VIPP1 in chloroplast envelope maintenance in Arabidopsis. *The Plant Cell* **2012,** 24, (9), 3695-707.

52. Adam, Z.; Rudella, A.; van Wijk, K. J., Recent advances in the study of Clp, FtsH and other proteases located in chloroplasts. *Current Opinion in Plant Biology* **2006,** 9, (3), 234-40.

53. Kim, J.; Rudella, A.; Ramirez Rodriguez, V.; Zybailov, B.; Olinares, P. D.; van Wijk, K. J., Subunits of the plastid ClpPR protease complex have differential contributions to embryogenesis, plastid biogenesis, and plant development in Arabidopsis. *The Plant Cell* **2009,** 21, (6), 1669-92.

54. Finley, D., Recognition and processing of ubiquitin-protein conjugates by the proteasome. *Annual Review of Biochemistry* **2009,** 78, 477-513.

55. Vierstra, R., The ubiquitin/26S proteasome pathway, the complex last chapter in the life of many plant proteins. *Trends in Plant Science* **2003,** 8, (3), 135-142.

56. Wang, L.; Ouyang, M.; Li, Q.; Zou, M.; Guo, J.; Ma, J.; Lu, C.; Zhang, L., The Arabidopsis chloroplast ribosome recycling factor is essential for embryogenesis and chloroplast biogenesis. *Plant Molecular Biology* **2010,** 74, (1-2), 47-59.

57. Koumoto, Y.; Shimada, T.; Kondo, M.; Hara-Nishimura, I.; Nishimura, M., Chloroplasts have a novel Cpn10 in addition to Cpn20 as co-chaperonins in Arabidopsis thaliana. *The Journal of Biological Chemistry* **2001,** 276, (32), 29688-94.

58. Xu, Y.; Wang, B. C.; Zhu, Y. X., Identification of proteins expressed at extremely low level in Arabidopsis leaves. *Biochemical and Biophysical Research Communications* **2007,** 358, (3), 808-12.

59. Fulton, D. C.; Stettler, M.; Mettler, T.; Vaughan, C. K.; Li, J.; Francisco, P.; Gil, M.; Reinhold, H.; Eicke, S.; Messerli, G.; Dorken, G.; Halliday, K.; Smith, A. M.; Smith, S. M.; Zeeman, S. C., Beta-AMYLASE4, a noncatalytic protein required for starch breakdown, acts upstream of three active beta-amylases in Arabidopsis chloroplasts. *The Plant cell* **2008**, 20, (4), 1040-58.

60. Ren, Y.; Yang, J.; Lu, B.; Jiang, Y.; Chen, H.; Hong, Y.; Wu, B.; Miao, Y., Structure of Pigment Metabolic Pathways and Their Contributions to White Tepal Color Formation of Chinese Narcissus tazetta var. chinensis cv Jinzhanyintai. *International Journal of Molecular Sciences* **2017,** 18, (9).

61. Shao, L.; Shu, Z.; Peng, C. L.; Lin, Z. F.; Yang, C. W.; Gu, Q., Enhanced sensitivity of Arabidopsis anthocyanin mutants to photooxidation: a study with fluorescence imaging. *Function Plant Biology* **2008,** 35, (8), 714-724.

62. Carpentier, S. C.; Witters, E.; Laukens, K.; Deckers, P.; Swennen, R.; Panis, B., Preparation of protein extracts from recalcitrant plant tissues: an evaluation of different methods for two-dimensional gel electrophoresis analysis. *Proteomics* **2005,** 5, (10), 2497-507.

63. Bradford, M. M., A rapid and sensitive method for the quantitation of microgram quantities of protein utilizing the principle of protein-dye binding. *Analytical Biochemistry* **1976,** 72, 248-54.

64. Wang, L.; Pan, D.; Li, J.; Tan, F.; Hoffmann-Benning, S.; Liang, W.; Chen, W., Proteomic analysis of changes in the *Kandelia candel* chloroplast proteins reveals pathways associated with salt tolerance. *Plant Science* **2015,** 231, 159-72.

65. Fling, S. P.; Gregerson, D. S., Peptide and protein molecular weight determination by electrophoresis using a high-molarity tris buffer system without urea. *Analytical Biochemistry* **1986,** 155, (1), 83-8.

Peer-reviewed version available at Int. J. Mol. Sci. 2018, 19, 2231; doi:10.3390/ijms19082231

719 Supplemental Table S1 The list of primer pair sequence for qRT-PCR

TAIR number	Gene name	Primer sequences（5’ to 3’）
At1g14410	WHIRLY1	FP: TTTTACGTGGGTCATTCGAT RP: GTCCACTGTTAACGCAGCTT
At2g02740	WHIRLY3	FP: ACGGTGAAGTCTCGACAAAG RP: ATCGAATGACCCACGTAAAA
AT5G01820	CIPK14	FP:TAGACACGAATCCGCAGACGA RP:TCGTCGTAGCCCTGTTTGAACC
AT1g13440	GAPC2	FP:ACCACTGTCCACTCTATCACTGA RP:TGAGGGATGGCAACACTTTCCC
AT3G24430	spot 1	FP:CACTTTGACGCTGATGGGAAACG RP:TGCCGAATTGCTTGACCACCTC
AT2G39730	spot 2	FP:AGACCGTATCGGTGTCTGCAAG RP:CCCTCAAAGCACCGAAGAAATCG
ATCG00120	spot 3	FP:TTCTTCCGTGGCTCAGGTAGTG RP:GGCCGTTTCAGCTACCACAATAG
AT5G45930	spot 4	FP:TGTGCTGAGCTGGACGTTGATG RP:AGCGCTCTAGCTGCTCTGTTTATC
AT3G12780	spot 5	FP:CGAGCTTCTTGGTATTGAGGTCAC RP:GGTAGAGAAGCCACCAAGCTTTCC
AT3G55800	spot 6	FP:TCGACAACTCCGAATACAGCAAGC RP:AACCATTCCTCCGGTGTATCGC
AT3G57260	spot 7	FP:AGCTTCCTTCTTCAACCACACAGC RP:TGGCAAGGTATCGCCTAGCATC
AT2G37220	spot 8	FP:GCTCAGCAGTTCAATGGCTATGAG RP:ACCATCTTCCCTCTTTGGTGGTG
AT5G54770	spot 9	FP:TTTCTCCGCCATGATTGTTCGC RP:AAGCCACACCAATCTCGTCAAGG
AT4G08390	spot 10	FP:TCTAGGCCAGAACGTAGTGGTTGG RP:TGCTCCAGGTCCTTCTTTCGTG
AT1G09130	spot 11	FP:TATGATGCCACATGCCAAAGCG RP:ACATCACTGGCAGGCATCAACC
AT4G10340	spot 12	FP:GCCGTAGTTGCTGAGGTTGTTC RP:AGCTTGTCCTCGAAATCCAATCCG
At5g35590	spot 13	FP:AGGTCGTCTCTTCCAAGTCGAG RP:TTCTGCGTAACGACGCATACTG
AT1G64510	spot 15	FP:CATGTCTGAAGATGAACGGCTTGG RP:TCCTGCCACAAGCAACTCTTCG
AT2G44650	spot 19	FP:GGACAACAAGTTGGACCTGGAAAG RP:CATCGGTTCCCAAATCGACCTC

720
721

Peer-reviewed version available at Int. J. Mol. Sci. 2018, 19, 2231; doi:10.3390/ijms19082231

TAIR number	Gene name	Primer sequences（5’ to 3’）
AT1G02930	spot 20	FP:AAGAGCCTTTCATCCTTCGCAACC RP:TGTCCTTGCCAGTTGAGAGAAGG
AT4G17090	spot 21	FP:AAAGCACGGTCTCAAACTCCAG RP:ACTGCAAGAGTCTCCTACGTTTCC
AT4G13930	spot 22	FP:AAAGCCAATGCTGTTGCCCTTG RP:CAGAGCTTCTCAACCTTGTTTCCG
AT4G11150	spot 24	FP:TGCGCGTCTTGATGTGGCATTC RP:GCCGAACAACGACTTACGGATCAC
AT1G07890	spot 25	FP:TTTCCACCCTGGAAGAGAGGAC RP:TGGTCACAACCCTTGGTAGCATC
AT4G25080	spot 26	FP:AGGAGCAATCGTCTCTGCTTCC RP:ATGGTAGTTGTGCCTTTGCCTTC
AT1G77090	spot 28	FP:CGAACCTGATGAAGAAGGTTGGAG RP:ACCAAGATCAGCGATCGATACAGG
AT4G14800	spot 29	FP:GGCGGATACATCAGCAGTTCACAG RP:TCCGTAAACTGAACCCGGTCAC
AT3G63190	spot 30	FP:GCGATGCTTGACAAGATTGAGGTG RP:CCGGAGTACTGATTTGGGCTATGC
AT4G38740	spot 31	FP:AGACGTGGTAAAGGCCATCGAG RP:ATCGGCAACAACCACAGGCTTC
AT4G05180	spot 33	FP:ACACCGTTATCTCCGCTAAGCC RP:TGATCTCGCCGCATAGTCCAAG
AT1G79040	spot 34	FP:TAACGGCAGCATGGACTTGAGG RP:ACTTGTAAACACCGTATCCCTTGC
AT4G01050	spot 35	FP:ACCAACCGAAACAGAAGCCAAAC RP:ATGGAGGCTTCAAGTCAGGGTACG
AT3G47520	spot 36	FP:GCTCACTGTTAGGATTCAGAACGC RP:AACCTGCACCTGCCTTAGCATC
AT2G38230	spot 37	FP:AAGGCGGTGTTGCTCGAATGAG RP:TTTCGCCATCACCGGAATCGTC
AT1G76080	spot 38	FP:TTCTTGCTCGTCATGGGTGATG RP:CTGGTCCGGTTCAATACCTTCTTC
AT2G05840	spot 39	FP:AGGTCGTCTCTTCCAAGTCGAG RP:TTCTGCGTAACGACGCATACTG
AT2G21660	spot 44	FP:TCAATGGCGTCCGGTGATGTTG RP:TCATCAGTGGCCCATGCTAGAC
AT3G01390	spot 46	FP:AGAGGAAACTTGAGGAGACAAGC RP:CTTGCTCCAGCCTCTTCACATTCG

722

723

TAIR number	Gene name	Primer sequences（5’ to 3’）
AT5G11670	spot 47	FP:GGACCTCATTGGTGCTGTTAATGC RP:CCACACCGGATGTTCCAATGAG
AT5G65010	spot 48	FP:TGTCTTCCCGGATAACACACCTC RP:AGTCGCTCTAGCAGCACTCTTC
AT3G47930	spot 49	FP:GGCCACCTAAGGACAAACCAAAG RP:CCTGGACCCTATACTTCACAATGC
AT1G23310	spot 50	FP:TTACCAACGGGAGCTCTCCAAG RP:GTTGTCCTCAGATGGAACACACC
AT5G14780	spot 51	FP:AAGGAAGGCCCTGATTGCGAAC RP:AAGGGAGTGGAGATTAGGACGTG
AT2G06050	spot 52	FP:ACGTGCTTCTCATGCAGTGTATC RP:TACTTCACGTGGGAACCATCGG
AT1G29670	spot 53	FP:AGAAGAAACCGGTCGACAATTGGG RP:GCTGCACAACTTGCGATACTGTG
AT4G09010	spot 54	FP:GCATATGGTTCAGCTGGTCAGTGG RP:TCAGCCTCTGTTGCATCACTCC
AT2G45820	spot 55	FP:TCTGGTTCGGCCGATAGAGATG RP:TTCCCAAGCATGCACATCAGAG
AT2G16600	spot 56	FP:ACATGACCGTCGGTGGCAAATC RP:TTCTCGGCGGTTTCTGGTGTTG
AT1G65260	spot 57	FP:TCTTGCACGTGAGGCCCTTAAAC RP:TTCAAAGCAGTAGCGTTGTCAGC
AT3G57560	spot 58	FP:ATACAGTTGCTGGAGAGCTTGCG RP:TTCCAGCCACATCAGTCAGCAG
AT3G01500	spot 59	FP:AGATGCCTTCGTGGTCCGTAAC RP:CAACGCCACCGTATTTGACCTTG
AT1G02920	spot 60	FP:AGCCTTTCATCTTCCGCAACCC RP:TTGGAGCCAAGGGAGACAAGTTGG
AT4G25130	spot 61	FP:ACTGGCACTACGGGACATAACG RP:ACCCTGACGATTCAAGGTGGTTG
AT1G73230	spot 62	FP:ATCAGCCAACTTGGACCAGATAAC RP:ACCTGGAGCTTGTTTCTGGAATTG

724

725